Marco Roy

Photofunctionalization of titanium surface

Promotor :

Prof. dr hab. Wieslaw Hedzelek

Poznan University of Medical Sciences,

im. K. Marcinkowskiego

Prosthodontics Department

Poznan 2018

CONTENTS

ABBREVIATIONS:

BIC: the percentage of dental implant surface covered by newly formed bone, is one of the critical measurements used to quantify the degree of osseointegration.

Ti-6Al-4V: Titanium alloy used in the medical field to produce a biomaterial which improves the mechanical characteristics of Titanium. It contains around 6 wt% aluminium and 4 wt% vanadium.

UV: is an electromagnetic radiation with a wavelength from 10 nm to 400 nm, shorter than that of visible light but longer than X-rays. UV radiation constitutes about 10% of the total light output of the Sun, and is thus present in sunlight.

XPS: It stands for X-ray photospectroscopy. It is a surface-sensitive quantitative spectroscopic technique that measures the elemental composition at the parts per thousand range, empirical formula, chemical state and electronic state of the elements that exist within a material. XPS spectra are obtained by irradiating a material with a beam of X-rays while simultaneously measuring the kinetic energy and number of electrons that escape from the top 0 to 10 nm of the material being analyzed. XPS requires ultra-high vacuum (UHV; $P < 10^{-9}$ millibar) conditions.

AES: Auger electron spectroscopy is a common analytical technique used specifically in the study of surfaces and, more generally, in the area of materials science. Underlying the spectroscopic technique is the Auger effect, as it has come to be called, which is based on the analysis of energetic electrons emitted from an excited atom after a series of internal relaxation events.

SEM: A scanning electron microscope is a type of electron microscope that produces images of a sample by scanning the surface with a focused beam of electrons. The electrons interact with atoms in the sample, producing various signals that contain information about the sample's surface topography and composition.

AFM: Atomic-force microscopy is a type of scanning probe microscopy, with resolution on the order of fractions of a nanometer, more than 1000 times better than the optical diffraction limit.

EDS: Energy-dispersive X-ray spectroscopy, is an analytical technique used for the elemental analysis or chemical characterization of a sample. It relies on an interaction of some source of X-ray excitation and a sample. Its characterization capabilities are due in large part to the fundamental principle that each element has a unique atomic structure allowing a unique set of peaks on its electromagnetic emission spectrum

RT-PCR: A **real-time polymerase chain reaction**, also known as quantitative polymerase chain reaction (qPCR), is a laboratory technique of molecular biology based on the polymerase chain reaction (PCR). It monitors the amplification of a targeted DNA molecule during the

PCR, i.e. in real-time, and not at its end, as in conventional PCR. Real-time PCR can be used quantitatively (quantitative real-time PCR), and semi-quantitatively

1.INTRODUCTION

1.1 DENTAL IMPLANTOLOGY BACKGROUND

Dental implantology, a field of dentistry, has become a standard in dental restorative treatment to restore lost function and aesthetics in edentulous and partially edentulous patients[1]. Dental implants aim to simulate the root-crown apparatus in the most physiological manner, being inserted into the root-bearing parts of the mandible or maxilla and a prosthetic restoration on top either screw retained or cemented. However, current implant therapies cannot be defined as being optimal considering the protracted healing time and limitations dictated by bone anatomy, systemic factors, smoking and ageing. According to Lee et al [2] the survival rate for an implant today is around 92% over a period of 5 years, while in a period of 10-15 years Norowski et al [3] report it to be around 89%, though the dental infection risk may be as high as 14%. Bacterial colonization on an implant could lead to inflammatory reactions and loss of osteointegration. A major limitation of clinical success is peri-implantitis, an inflammatory process that attacks the soft and hard tissues around the implant [4] . Researchers, clinicians and manufacturers have made it possible to improve the chemical and topographical aspects of titanium to improve the biological principles underlying osteointegration [5]. Different chemical and physical approaches, (abrasion, anodization, acid etching, plasma spraying) have been used in an effort to improve the surface properties of implant materials. To guarantee the stability and long life of an implant, good bone anchorage needs to be achieved, in other words, the stability is dependent on the so-called bone-implant-contact (BIC). Nevertheless, the BIC range value is generally between 45%± 16%, far below the ideal 100% mark. To increase the long term success rate, it is imperative to enhance the integration between biocompatible materials and soft and hard tissues. Ideally it should increase the activity of cells that in turn, increase the speed of the healing process/osteointegration.

1.2 PROCESS OF OSTEOINTEGRATION

The process of integration of a dental implant with bone has been defined overall as the process of osseointegration. The term was suggest by Branemark in 1969 [6], originally defined as a direct deposition of bone on the implant surface. This concept has been described by Brånemark as consisting of a highly differentiated tissue making a direct structural and functional connection between ordered, living bone and the surface of a load-carrying implant.

Since then more definitions have been provided, Albrektsson et al.[7] described it as: "a direct functional and structural connection between living bone and the surface of a carrying implant". Subsequently, a more clinical definition was provided by Zarb and Alberktsson in 1991 referring to osteointegration as "a process whereby clinically asymptomatic rigid fixation of alloplastic materials is achieved and maintained in bone during functional loading". Another term used to describe the process was provided by Schroeder et al [8] that is "functional ankylosis". They stated that: new bone is laid down directly upon the implant surface, provided that the rules for atraumatic implant placement are followed and the implant exhibits primary stability. Many experimental studies were performed to describe and understand the steps involved in bone formation and osseointegration of the implants.

Bone healing around dental implants is activated by any lesion of the pre-existing bone matrix. As in direct bone healing (primary fracture healing) a cascade of cellular and extracellular biological events take place at the bone implant interface until the implant surface appears finally covered with newly-formed bone [9].The sequence of events includes the activation of osteogenic processes, which are regulated by growth and differentiation factors released by the activated blood cells at the implant surface [10]. Immediately following implant placement, non-collagenous proteins and growth factors are released and activate bone repair. Attracted by chemotaxis, osteoprogenitor cells of the bone marrow and from the endocortical and periosteal bone envelopes migrate into the site of the lesion [11]. They proliferate and differentiate into osteoblast precursors and osteoblasts, and start depositing bone-related proteins and creating a non-collagenous matrix layer on the implant surface that regulates cell adhesion [12] [13]. Already after 4 to 6 weeks after implantation there is and early deposition of new calcified matrix on the implant surface called woven bone. It is often considered as a primitive type of bone tissue and characterized by random collagen fibrils, numerous and irregularly shaped osteocytes and a relatively low mineral density. Woven bone fills the initial

gap at the implant-bone interface. Arranged in a three-dimensional regular network, ensuring biological fixation and high resistance to early implant loading [14, 15].

Starting in the second month, woven bone is progressively remodeled and substituted by lamellar bone that may reach a high degree of mineralization [16]. As far as the growth pattern is concerned, lamellar bone cannot form a scaffold like woven bone, but merely grows by apposition on a preformed solid base [11]. At three months post-implantation, a mixed bone texture of woven and lamellar matrix can be found around the implant [17]. The last stage of osteointegration comprising bone remodeling starts around the third month and contributes to the adaptation of bone structure to stress and mechanical loading. The turnover of peri-implant bone is characterized by the presence of medullary or marrow spaces containing osteoclasts, osteoblasts, mesenchymal cells and lymphatic/blood vessels next to the implant surface [14, 17]. This process improves bone quality and functional adaptation either by replacing pre-existing, necrotic bone and/or initially formed, woven bone with mature, viable lamellar bone or by changing the dimension and orientation of the supporting elements [11]. Bone remodeling continues throughout life, preventing the accumulation of micro-damage and fatigue of bone, and thus ensuring the longevity of the implant [18].

However, the interaction between the living tissue and the implant can be affected by systemic and local factors, which are summarized in ***TABLE 1***

Factors enhancing osseointegration	Factors inhibiting osseointegration
Implant design, shape and diameter	Excessive implant mobility and micromotion
Titanium coating on Co-Cr metal implant	Nonsteroid anti-inflammatory drugs especially COX-2 inhibitors
Laser treatment of implant surface	Warfarin and low molecular weight heparin
Human PTH (1-34)	Inappropriate porosity of the porous coating of the implant
Osteogenic transcription factors	Osteoporosis, rheumatoid arthritis
Local delivery of transcription factors	Radiation therapy
Bone source augmentation to socket	Smoking
Mechanical stability and loading conditions applied to the implant	Advanced age, nutritional deficiency and renal insufficiency
Pharmacological agents such as simvastatin	Pharmacological agents such as cyclosporine A, methotrexate and cis-platinum

Table 1 Factors involved in increase and inhibition of osseointegration [19]

1.3 BIOMATERIALS IN DENTAL IMPLANTOLOGY

A biomaterial is defined as a natural or synthetic material that can be used in a living body to replace parts or functions in a reliable, safe and physiologically acceptable manner; to maintain or improve the quality of life [20] [21, 22]. The most widely used materials for dental implants are Titanium (and its alloys) and Zirconium oxide[23]. The Williams dictionary of biomaterials defined also the term biocompatibility, as "the ability of a material to perform with an appropriate host response in a specific situation"[20]. In other words, a biomaterial should not induce any harmful effect being non-toxic, non-immunogenic and non-carcinogenic. TiO_2 and ZrO_2 are both oxides and have the same stoichiometry. In fact they both belong to the 4^{th} group of the periodic table, and their chemical characteristics are thus similar. TiO_2 and ZrO_2 surfaces present themselves with slightly different interatomic distances. However, to the present the mechanical properties of ZrO_2 are not quite as good as those of TiO_2. Both materials have been used for the production of dental implants. However to be sufficiently rigid and usable in the clinical practice the ZrO_2 implants are produced as a one piece elements reducing considerably their versatility during the restorative phase of treatment. Taking into account available literature a number of systematic reviews have commented on the scarcity of clinical data supporting the use of zirconia implants which are mainly limited to cohort investigations of lower evidential value [24, 25]. The recent work of Reham et al. discourages the use of these implants for the rehabilitation for anything other than a single tooth, due to the increase of marginal bone loss and higher fracture rate when compared to titanium implants and concluded that their use should be limited to cases with a proven allergy to titanium [26]. From an aesthetic point of view ZrO_2 presents great advantages especially in patients with a thin gingival biotype and for this reason it is usually utilized for dental abutments. Overall, the amount of ZrO_2 implants utilized in the worldwide market is about 5%. All considered, titanium still remains to date the material of choice for dental implants, therefore this thesis is not going to address any other implantable material

The main advantage of titanium is its high strength-to-weight ratio. Its strength is comparable to steel, but the density is just half of it. It also possesses good mechanical properties and corrosion resistance, which is maintained even at high temperature [27]. The conventional titanium alloys have a yield strength in the range of 800-1200 MPa and a Young's modulus of around 100-140 GPa. In the medical field, the most commonly used titanium alloy is Ti-6Al-4V. As the name says, it contains around 6 wt% aluminum and 4 wt% vanadium. To show its advantages, a comparison of the mechanical properties of Ti-6Al-4V and commercial pure titanium (Grade2) can be seen in **TABLE 2** On titanium, a stable, dense, non-conductive oxide film is formed, which prevents the flow of ions making it a biocompatible material [28, 29]. The advantage of titanium and its alloys for load bearing orthopedic implants is its low Young's modulus [27]. Its value is the closest to the Young's modulus of bone among all metallic biomaterials, which therefore gives better transfer of the load and, thus, stimulates bone growth [29].

Table 2 Comparison of mechanical properties of Ti and Ti-6Al-4V at room temperature

Property	***Ti***	***Ti-6Al-4V***
Ultimate tensile strength *(MPa)*	240-330	900-990
Yield strength *(MPa)*	170-240	830-920
Elongation *(%)*	30	14
Reduction in area *(%)*	55	30

1.3.2 TITANIUM OXIDES CHEMICAL COMPOSITION

Titanium is a transition metal, it has several available chemical states and may form very stable oxide films. The most common oxidation state of titanium is Ti^{4+} (TiO_2), but lower states such as Ti^{3+} (Ti_2O_3) and Ti^{2+} (TiO) may also occur [30]. It is possible to distinguish between 3 different crystal structures of titanium oxides, anatase (tetragonal), rutile(tetragonal) and brookite (orthorhombic)[30]. Due to the high affinity between oxygen and titanium, an oxide layer is easily formed on its surface [30]. The process of oxidation is shown in **FIG 1**. Firstly, the oxygen forms a monolayer on the surface (panel b), then the oxide is formed by diffusion of the oxygen atoms into the material and/or metal ion diffusion onto the surface (panel c) [30]. After the nucleation, the oxide grows laterally to cover the whole surface (panel c) [31]. Then the oxide film grows in thickness, and the diffusion rate of the atoms and ions will decrease until it becomes zero and the growth then stops (panel d) [30]. The oxide film formed protects the surface from further oxidation, only in case of damage, it can spontaneously react with oxygen or water present in the environment for self-reparation [32]. Typically the oxide layer formed in the atmosphere has a thickness of about 5-10nm [32] and is composed of a mixed crystal structure of anatase and rutile [33] [34]. As stated earlier in the medical field titanium is frequently used as an alloy, most commonly Ti-6Al-4V. The oxide formed in this alloy has a different composition and morphology than that of the pure metal. The presence of aluminum in the alloy makes it possible to detect Al_2O_3 oxide on the surface. However, the TiO_2 is equally stable and thus inhibits the growth of aluminum oxide. On the other hand, Vanadium cannot be detected on the outermost surface, only after removal of the oxide layer it can be detected with XPS and AES analysis mainly in the form of V_2O_5 [30].

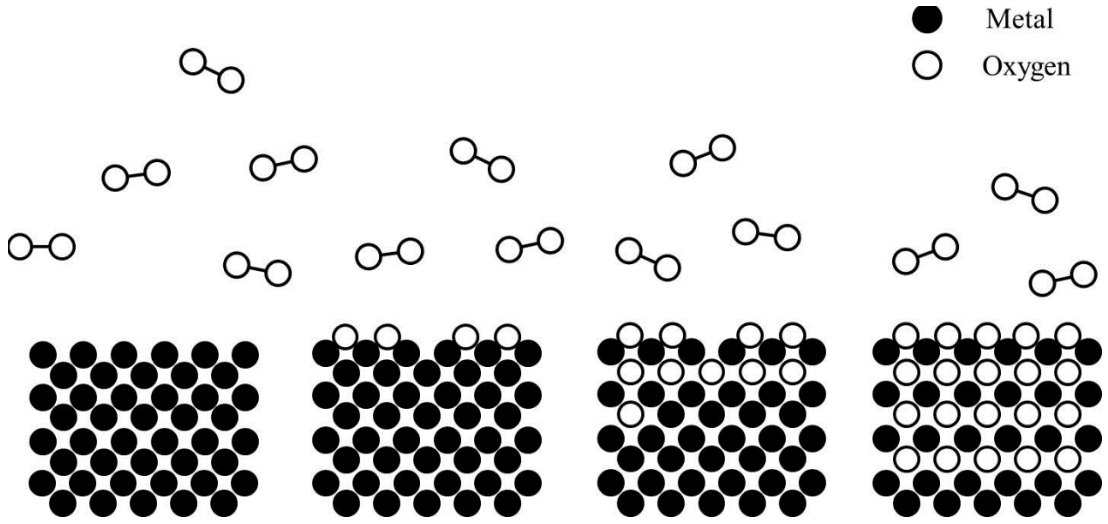

Figure 1 Formation of oxide on a metal surface Adapted from [35]

1.4 TITANIUM SURFACE TOPOGRAPHY AND TREATMENT TO IMPROVE OSTEOINTEGRATION

1.4.1 TOPOGRAPHY AND CHARACTERISTIC OF IMPLANT SURFACES

Implant surface topography namely, macroscopic, microscopic and nanometric characteristics are considered some of the most important factors in osseointegration. Roughing of the surface has been proven to increase osteoblastic proliferation, differentiation and adhesion, whilst fibroblast adhesion seems to be weaker[36, 37]. Implant surface roughness is divided into 3 subgroups: macro, micro and nano roughness.

- Macro roughness, has a range between millimeters and microns, it is involved in the implant geometry of the threads and its macro porousness. The interlocking of these structure with the bone is responsible for the initial implant stability [38]. A major risk with high surface roughness may be an increase in peri-implantitis as well as an increase in ionic leakage [39].

- Micro roughness, has a range from 1-10 microns. This topography is responsible for the interlocking of the bone at the implant interface [40]. Studies supported by some clinical evidence suggest that the micron-level surface topography results in greater bone-to-implant contact and higher resistance to torque removal than other types of surface topography [38]. In animal studies, a moderately rough surface with a Sa of about 1,5 μm promotes the strongest bone response [41-43]. Therefore, it has been pointed out that a major indication for using an implant with a rough surface is in conditions of poor bone quality or volume. In these unfavorable clinical conditions, early and high bone-to-implant contact would be beneficial for allowing a high level of loading [44]. In this context, it should be mentioned that micro-rough surfaces have been generally interpreted as biocompatible with limited ability to directly affect the initial response of surrounding tissues, i..e., the ability to enhance bone formation or to prevent bone resorption[45].

- Nano Roughness, is related to nano-sized materials with a size of 1-100 nm on the implant surface. This microscopic roughness is believed to increase the surface energy which in turn increases the wettability and in turn promotes absorption of proteins and adhesion of osteoblasts [46]. It should be pointed out that, reproducible surface roughness in the nanometer range is difficult to produce with chemical treatments. In addition, the optimal surface nano-topography for selective adsorption of proteins leading to the adhesion of osteoblastic cells and rapid bone apposition is unknown.

The implant surface can be modified by mechanical means namely, grind blasting, machining and polishing. Chemical treatment with acid or alkali, sol gel, hydrogen peroxide treatment, anodization and chemical vapor deposition are other valid methods to alter the surface roughness and composition. In addition physical methods like plasma spraying, ion deposition and sputtering have also been used to modify the surface. Here will follow a description only for machined, sand blasted and acid etched modified surfaces being the ones used for the samples used during the investigation.

Machined surface.

Used in the first generation of dental implants. They were considered smooth but if analyzed under the scanning electron microscope grooves and ridges created during manufacturing can be appreciated. The disadvantages of this surface is the inability of the fixture to interlock with bone therefore creating a delay in osteointegration [40].

Etched surface

Acid etching is performed with strong acids, typically a mixture of HNO_3 and HF or a mixture of HCl and H_2SO_4. The process is able to remove the oxide layer on the surface in addition to some parts of the underlying material. The effect is the creation of homogenous irregularities known as micro pits with sizes ranging from to 0.5 to 2 µm in diameter. As a result the surface area is increased and bio-adhesion is enhanced. A more rapid osteointegration with long-term success has been reported when titanium surface was roughened by acids [40]. Also introduced and used is a technique called dual etched, which is the immersion of the titanium surface for several minutes in a mixture of concentrated HCl and H_2SO_4 heated above 100°C. It has been speculated that this treatment can achieve a specific topography, which makes it possible for fibrin to attach and in turn guide the osteoblasts, hence promote bone apposition[47].

Sand-blasted surface

Machined surfaces can be sand-blasted with 0.25-0.50 µm titanium dioxide particles giving roughness to the surface. The implants which underwent this type of modification have been reported to have a higher success rate than unblasted implants [48]. Alumina (Al_2O_3) is frequently used as a blasting material and produces surface roughness varying with the granulometry of the blasting media. However, the blasting material is often embedded into the implant surface and residue may remain even after ultrasonic cleaning, acid passivation and sterilization. Alumina is insoluble in acid and is thus hard to remove from the titanium surface. Is some cases, these particles have been released into the surrounding tissues and have interfered with the osseointegration of the implants [49]. Comparative clinical studies have given higher marginal bone levels and survival rates for TiO_2 grit-blasted implants than for machined turned implants [50]. This surface treatment is still used by some manufacturers but it most of the cases it has been the starting point for a more effective surface treatment which is sandblasted and acid etched.

Sandblasted and acid-etched surface

In the last few years a new protocol has been introduced which exploits both sand blasting with large grit particles 250-500 μm followed by etching with acids. As a result macrostructures are created after sand-blasting and in addition thanks to acid etching also micro-irregularities are created. The healing process seems to be faster and this type of modification is recommended when an immediate loading is planned [51].

1.4.2 HYDROPHILICITY OF IMPLANT SURFACES

In addition to topography the hydrophilic nature of a material's surface is a representative marker for surface energy and may play an important role in their interaction with biological molecules, cells and tissues [52]. The biological response is greatly affected by the surface free energy and hydrophilicity. In the initial phase of osseointegration, surface energy and hydrophilicity have been shown to alter the extent of protein adsorption [53]. In other words, the exact mixture of proteins on the surface and their conformational state(s) will be different, depending on the original surface properties, e.g., how the surface binds water [54]. The latter lies behind the common observation that, for example, hydrophilic and hydrophobic surfaces bind proteins differently [52]. It is well-established that fewer proteins tend to adhere to hydrophobic surfaces and they bind less tightly than to hydrophilic surfaces [55-57]. Moreover, on very hydrophilic surfaces, it is more likely that proteins bind with their hydrophilic areas toward the surface, and with intact water shells, while on very hydrophobic surfaces, the proteins are more likely to bind with their hydrophobic segments closest to the surface, and without intervening water shells [52]. The structure and state of a such protein layer is thought to be responsible for cell-surface interactions. Immediately after implantation, biomaterials are covered with a layer of plasma proteins, predominately albumin, fibrinogen, IgG, fibronectin, and von Willebrand factor [58-60]. The amount and composition, as well as the degree of the

conformational state of the absorbed proteins, regulates the cellular response [61]. It is believed that these proteins: through biomaterial interactions prompts the exposure of hidden protein structures and sequences that serve as receptor sites for different types of cells, which then initiate the body's reactions to the implant material surface.

1.5 UVC IRRADIATION TO INDUCE THE PHOTOCATYLITIC EFFECT

It has been reported by some researchers that the titanium used for manufacturing dental implants changes over time, undergoing physical modifications namely an increase of carbon is detected onto its surface. The titanium surface constantly attracts organic impurities, such as polycarbonyls and hydrocarbons from the atmosphere, water, and cleaning solutions used during the final decontamination of the implants before packaging [62-65]. The contamination with hydrocarbons of the titanium surfaces is reported to be a physiological phenomenon, described as biological aging [63, 66-69]. The amount of carbon is known to vary depending upon the age of surfaces and reportedly can increase from 20% on freshly produced titanium to approximately 60–75% at 4 weeks after production biological ageing [1, 70].

The presence of carbon plays a key role on the wettability of the surface, from hydrophilic – when the fixture is produced – to hydrophobic – over the 4 weeks after production. This phenomenon could create a coat around the surface and lead to an insufficient attraction of stem/progenitor cells, resulting into an incomplete osteointegration of the implants. A newly introduced procedure, termed UV photofunctionalization, has attracted considerable attention and interest; it has been reported as a method to modify the surface and increase its biological capability reducing the amount of contamination. Ultraviolet light (UV), corresponds to electric magnetic radiation with 100-400nm wavelength fig. 2. Even though they are divided into UVA, UVB and UVC depending on the wavelength, all the studies have been using a wavelength 100-280 nm corresponding to UVC fig. 2. Such effect is not completely unknown as, since 1969, the ability of the UVC wavelength in cleaning the TiO_2 coated materials has been demonstrated in other industrial field, like the photovoltaic. [71]. The UV absorption excites an electron from the valence band to the conduction band of the semiconductor. The resulting excited electrons, in the otherwise empty conduction band, and the "positive hole" in the valence band allow charge transfer to the TiO_2 surface which facilitates oxidation of

surrounding molecules. Sometimes direct charge transfer causes the oxidation [72]. Alternatively, hydroxyl radicals, formed by the "positive holes" in the valence band accepting electrons from hydroxyl ions, are catalytically active intermediates [72]. This phenomenon is the starting point of the process of photofunctionalization.

Many in vitro studies were performed to analyze the behavior of TiO_2 after UV irradiation, mainly focusing on the behavior of animal and human osteoblasts, as well as of periosteum-derived osteogenic cells [73-76]. Ogawa et al. studied the effects of UV irradiation on titanium discs of multiple surface topographies. Sand-blasted, acid etched, machined, and nanofeatured treatments were used to simulate the different characteristics of the implants produced. A cell line of pre-osteoblasts (MC3T3) cultured on UV treated surfaces showed better attachment and increased cell proliferation, increased protein adsorption and enhanced osteoblastic differentiation, as compared to control cells grown on untreated surfaces [77]- However, the differences between treated and non-treated surfaces was evaluated at short time intervals, usually no longer than 48 hours. Enhancement in osteoblastic adhesion and growth in such a small window of time is anyway postulated to improve the implants outcome. In the study by Iwasa et al. two tests were performed to evaluate the early and successful cell attachment to titanium disks: a mechanical test using vibrational force, and an enzymatic one by trypsin treatment [78]. Both tests were performed after 3 and 24 hours of incubation of cells on the titanium surfaces. The results show that after the UV treatment the cell detachment was decreased by 110–120% after 3 hours incubation, and 50–60% after 24 hours. The conclusion was drawn that the UV treatment accelerates cell adhesion and increases the strength of adhesion [78]. It was pointed out that histologically there are differences between the osteoblasts cultured on the titanium surfaces; fluorescent images with actin filaments stain revealed that cells cultured on UV treated surfaces were enlarged with well-developed, philopodia-like cell processes, while cells remained small and circular on untreated surfaces [75]. Cytomorphometric evaluations of area, perimeter and Ferets diameter showed that the perimeter was 6 times greater and the cells area was 3,5 times greater on the UV treated surfaces [75]. Moreover, there was a greater expression of vinculin, a membrane- cytoskeletal protein involved in focal adhesion, suggesting that the cells settled faster and with higher strength on the UV treated surfaces [77, 78].

Albumin and fibronectin adsorption capacity is a useful parameter used to show the interaction between cells and proteins adsorbed on material surfaces [77]. Therefore their adsorption was studied after 6 and 24 hrs on titanium disks with different topographies before and after UV

irradiation [74]. According to Hori et al. the increase in protein adsorption was 80–300% for the UV treated disks as compared to non-treated, regardless of the specimen topography [74, 77].

To further investigate the way the UV irradiated titanium affects the rate of osteoblastic activity, additional biological markers, such as alkaline phosphate activity and calcium ion deposition and the expression of osteoblastic genes, were compared between the UV treated and not-treated surfaces. The results showed an increase of biological markers on the treated surfaces, suggesting a higher degree of cellular activity [62, 64, 74, 79, 80].

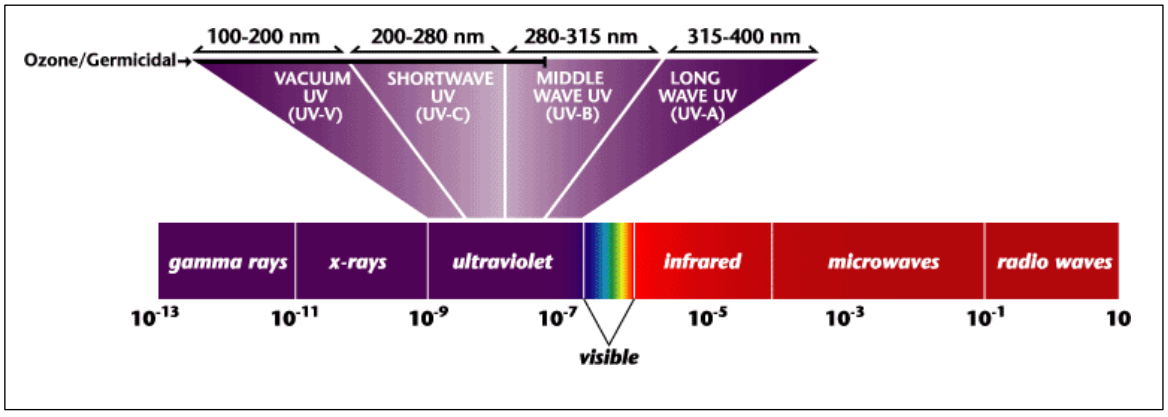

Figure 2 Electromagnetic spectrum of radiation. UV radiation is part of the not visible light with wavelength between 100-400 nm

In recent years Mesenchymal Stromal Cells, also called Mesenchymal Stem Cells, have raised great interest for their properties and characteristics as potential therapeutical tools for a wide spectrum of pathologies [81]. They are located in several easily accessible tissues, such as bone marrow, dental pulp, adipose and dermal tissues. Furthermore, following tissue damage they are selectively recruited to the sites that need repair, where they can secrete bioactive factors that inhibit scarring and apoptosis and stimulate angiogenesis and proliferation of endogenous stem/progenitor cells [82]. Therefore, MSCs may contribute to tissue repair either as multipotent cells or as trophic mediators. They can grow *ex vivo* and differentiate *in vivo* and *in vitro* into multiple phenotypes, including bone, cartilage, muscle, adipose tissue and hematopoietic-supporting stroma. Although they have not been isolated as a pure population, they can be separated from hematopoietic cells through repeated adhesion to plastic and selected on the basis of positive (CD90, CD105, CD106, CD73, CD166, SSEA-4, Stro-1 e SH-4) and negative (CD45, CD34, CD25, CD14, CD4 e HLA-DR) markers. However MSCs are intrinsically a heterogeneous population, with respect to embryonic origin and abilities to self-renew and differentiate. MSCs are rare and their quantity changes during lifetime , declining with age. What controls the number of MSCs in the marrow and why these numbers appear to change with age is not yet known. The capacity to self-renew relates to the rate of tissue turnover. While skin turns over every 30 days, the whole skeleton only turns over 3-5 times during adulthood. Consequently, self-renewal of stem cells capable of reforming skeletal tissues would not be expected to involve the same number of cell division as for epidermal or hematopoietic stem cells.

Several aspects of their biology still need to be clarified, also in view of their optimal therapeutical use. For example, a number of studies have highlighted the important role of specific regulatory molecules (growth factors, receptors and transcription factors) on MSCs self-renewal, however they cannot be maintained *in vitro* indefinitely and stop growing after a finite number of passages. Moreover it is still debated whether MSCs cultured for long periods of time reflect and retain properties and characteristics of MSCs present *in vivo* or shortly grown *ex vivo* [83]. Much effort has been invested both in in vitro expanding and phenotypically characterizing MSCs, as well as in identifying factors involved in their regulation of proliferation and/or differentiation potential. The definition of the regulatory

network orchestrating self-renewal and commitment to a specific differentiation program has a great biological and clinical impact.

1.7 OSTEOGENESIS

Throughout life, bone is constantly remodeled through the processes of bone formation by osteoblasts and bone resorption by osteoclasts. Bone marrow MSCs can give rise not only to osteoblasts, but also to a range of other cell types, including adipocytes, chondrocytes and myoblasts. Among these potential fates, differentiation to the osteogenic and adipogenic lineages has particular relevance to the maintenance of normal bone homeostasis. In support of a reciprocal relationship, numerous in vitro experiments have demonstrated that factors that induce adipogenesis inhibit osteoblast formation and, likewise, factors that promote osteoblastogenesis inhibit adipocyte formation. In bone marrow, the differentiation fate of MSCs is largely determined by the expression of specific groups of transcription factors and Runx2 is the main determinant of MSC osteoblastogenesis. Bone formation is characterized by a sequence of events starting with the commitment of osteoprogenitor cells and their differentiation into pre-osteoblasts, and then into mature osteoblasts, whose function is synthesizing the bone matrix that becomes progressively mineralized. Although the commitment phase of MSCs differentiation is not well defined yet, it is well established that the transcription Runx2 (Runt-related transcription factor 2) plays a critical role in the commitment of multipotent mesenchymal cells to the osteoblastic lineage, and is required at early stages of osteoblast differentiation. Runx2 is thus considered a master gene of osteogenesis, is involved in the production of bone matrix proteins and is able to up-regulate the expression of many bone matrix protein genes, including type 1 collagen, osteopontin, bone sialoprotein and osteocalcin. Runx2 expression is down-regulated in the late stage of osteoblast maturation. Interestingly, at the end of the commitment phase, the newly formed pre-osteoblasts undergo an extensive proliferation, characterized by an increased alkaline phosphatase activity (ALP) and osteocalcin synthesis. Pre-osteoblast proliferation is then followed by growth arrest, and the selective expression of specific genes that characterize the differentiated osteoblast phenotype (ALP, osteocalcin etc)

1.8 AIM OF THE STUDY

Titanium Oxide sill is the gold standard material used for the production of dental implants. However, even though implant therapies have reached a good success rate, they have not been developed at optimal levels and still need to be improved, to overcome the limited osteointegration due to aging, bone anatomy, smoking and metabolic diseases. Therefore, extensive research activity has been focused on improving the surface bio-activity of TiO_2, by modifying its composition (grade of purity), its topography and/or its roughness through machine, sand blasting and acid treatments. Furthermore, it has been reported that dental implants undergo biological aging, namely a contamination of titanium surface with hydrocarbons, which reduces osteointegration process. In recent years, the use UVC irradiation (photofunctionalization) has been proposed as an efficient method (means) to decontaminate titanium surfaces.

However, many questions regarding chemo- physical aspects of TiO_2 implant surfaces, as well as the mechanism and effects of the photofunctionalization process, remain still open, and in thesis of this dissertation, some of these issues have been addressed.

The starting hypothesis is that UVC treatment is able to produce a carbon free surface independent of the type of titanium or topography. In order to test this view, specific aims of the study are:

- Characterization of dental implant surfaces, using complementary chemo-physical techniques, namely XPS and AES before and after UVC photofunctionalization at different surface depths.

- Gaining insights into the mechanisms that underlie biological ageing and the effects of UVC photofunctionalization in relation to surface carbon contamination.

- To analyze the biological effects of UVC irradiated TiO_2 surfaces on osteogenic cells, using in vitro cultures of osteogenic progenitors.

- A better understanding of the osteointegration processes following photofunctionalization, knowledge which could give the basis for a clinical trial.

2. MATERIALS AND METHODS

2.1 SAMPLES

In order to analyze the effect of photofunctionalization and show how its effectiveness is not surface dependent, more than one titanium oxide material was utilized in the study. To perform the surface analysis, commercially available dental implants were used (as described in 2.1.1). However, the biological studies must be performed on flat surfaces, thus titanium disks were produced (as described in 2.1.2). Before proceeding with the deposition of the cells the chemical composition of the discs was analyzed and compared to that of the dental implants.

2.1.1 TITANIUM DENTAL IMPLANTS

In the physico-chemical analysis, commercially available Osteoplant Base™ and Rapid™ (Osteoplant, Poznan Poland) titanium dental implants were used. Geometrically the Base implant is cylindrical and the Rapid being instead conical. The implant surface was treated by the factory according to their protocols (both sandblasted or acid-etched). The titanium utilized to produce the implants is commercially pure titanium grade 4 alloy Ti-6Al-4V Figure 3.

Figure 3 Example of a titanium dental implant (Osteoplant Base) used during the physiscs analysis

2.1.2 TITANIUM DISKS

Cells were cultured on disk-shaped, commercially pure titanium samples (10x2 mm). The surfaces were divided into 3 groups depending on their surface treatment, machined surface titanium grade 2, sand-blasted surface and acid etched surface grade 2 and grade 4. These last 2 surfaces were obtained with a blasting procedure with aluminum oxide particles (350-500 lm) followed by an acid-etching procedure. However, the specific process used to produce the surface is considered a company proprietary process.

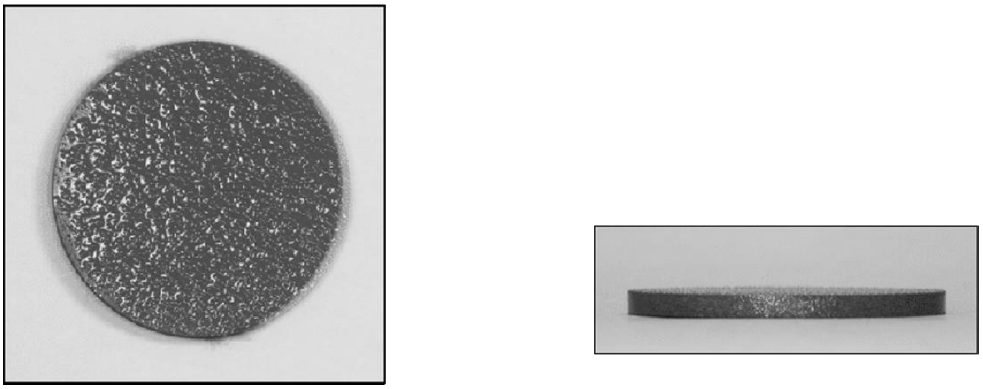

Figure 4 example of titanium disc used during the physical and biological studies. The disc is 10 mm in diameter and 2 in thickness.

2.3 UVC APPARATUS FOR PHOTOFUNCTIONALIZATION

The UV light was delivered to the samples with Therabeam Superosseo (Ushio) with cycles of 12 minutes. The implants/disks were placed on a dedicated tray to keep them in the middle of the light source figure 5

a)

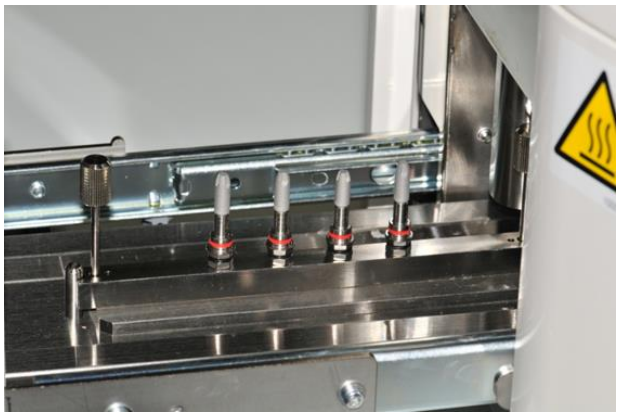

b)

Figure 5 UVC apparatus used to condition the samples: a) implants on stand after UVC photofunctionalization b) Ushio Therabeam Superosseo treatment

2.4 PHYSICAL-CHEMICAL ANALYSIS

2.4.1 SURFACE ANALYSIS, XPS, AES, EDS AND SEM.

Because more than one method was used to analyse the surfaces, first the differences between them should be clarified. In X-ray photoelectron spectroscopy (XPS) and Auger electron spectroscopy (AES), electrons emitted after the interaction between primary X-rays or electrons and a sample are detected. The amount of electrons that have escaped from the sample

without energy loss are typically measured in the range of 20 to 2000 eV. The data is represented as a graph of intensity versus electron energy. Due to the impact of the primary beam, the atoms in the sample are ionized, and electrons are liberated from the surface, either as a result of the photoemission process (XPS), or of the radiationless de-excitation in the Auger electron emission process (AES). Although XPS and AES are comparable methods in the sense that both are based on the use of a spectrometer to measure electrons of relatively low energy, the main difference between the two methods consists in the source of the primary radiation, which is necessary to provoke ionization of the atoms. AES makes use of an electron gun while XPS relies on soft X-rays. As a consequence of this, one of the main differences is the lateral resolution of the two methods. Since there is a continuous evolution in the design of the equipment and the performance of the techniques, it is difficult to express an absolute value for them. In our experiments with AES the lateral resolution was situated in the 10 to 100 nm range, while by means of XPS only a lateral resolution of a few to 100 µm was reached. In both methods low energy electrons are measured, giving rise to comparable depth and sensitivity values, which are respectively in the order of nanometers and of about 0.1 % atomic concentration. This type of measurements are necessarily performed under high vacuum conditions, and only samples restricted in size can be analyzed. From this point of view, XPS and AES cannot be considered as non-destructive techniques, although the analyses themselves are non destructive in nature. On the other hand, thanks to their spatial resolution, a small amount of material suffices for the analysis.

The implant surfaces, were studied by SEM (Scanning Electron Microscope), AES (Auger Electron Spectroscopy) and XPS (X-ray Photoelectron Spectroscopy) methods, in order to analyse the changes of surface morphology and chemistry. Measurements were performed with PHI5700/660 Physical Electronics spectrometer. SEM images were obtained at 10kV acceleration voltages and approximately ~20nA primary beam current. AES spectra were recorded in integral mode. Chemical distribution maps were obtained for carbon, titanium and oxygen. Photoelectron spectra were obtained with the use of a monochromatic Al anode x-ray source with energy $h\nu$ = 1486.8 eV of radiation K_α. Survey spectra and core lines of Ti2p, O1s, C1s, N1s and F1s were recorded. The Shirley type of background was subtracted before analysis. The fitting procedure was applied to the analysis of a shape of core lines by Seampik software. Moreover, atomic concentration of the elements was calculated from the auger and photoemission spectra by using the Multipak (Version 9.6.0.15) software.

The calculation of atomic concentrations with XPS and AES was based on relative peak intensities, modified using relative sensitivity factors (RSFs). Atomic concentration for each element was determined using the equation:

Atom % of element X = [(Ix/Sx) / (åIi/Si)] x 100

where Ix is intensity or peak area and Sx is the relative sensitivity factor for the element. Critical information including transmission function parameters and instrument configuration were stored with PHI XPS data files. Empirically derived relative sensitivity factors (ERSFs) and calculated average matrix relative sensitivity factors (AMRSFs) were both available in MultiPak for AES data reduction. More information can be found in the work by Seah [84].

To determine the mapping of the elements on titanium disks and prove that Carbon is spread all over the surface the X-ray dispersive spectroscope (EDS) technique was utilized; Mira III from Tescan coupled with electron X-ray dispersive spectroscope (EDS) Aztek Automated from Oxford Instruments.

2.4.2 CONTACT ANGLE (WETTABILITY)

The changes in wettability between the UV-irradiated and untreated titanium discs were analyzed by contact angle measurement. The water contact angle measurements were performed using a CAM101 goniometer with an accuracy of +/- 0,01°. The contact angles were determined in air using the static sessile drop method. Thirty images of water droplet ~15 µL placed on the surface were recorded during 30 s. Based on obtained images the average CA values were calculated. The final contact angle values were taken as the average of three measurements at different parts of surfaces. The measurements were repeated 3 times for each sample (n=3) calculating the angle created by 1µL H_20 and its surface. The sample was then stored for 4 weeks in the air before repeating the experiment.

2.4.3 AFM ANALYSIS

The topography of the Titanium implant was analysed by atomic force microscopy method. The study was performed with Solver P47 NT-MDT instrument worked in non-contact mode. The area of analysis of the samples was 50x50 µm and about 20x20 µm. Before the analysis the samples were cleaned in an isopropanol medium in ultrasonic washer.

2.5 BIOLOGICAL IN VITRO STUDIES

The biological studies have been divided into 2 phases; during the first phase Osteoblast-like cells MC3T3-E1 were utilized while in the second phase murine-MSC were used.

2.5.1 CELL CULTURE AND OSTEOBLAST DIFFERENTIATION

CELL CULTURES OF MURINE PRE-OSTEOBLASTIC MC3T3-E1 CELL LINE

Stock MC3T3-E1 cells were recovered from liquid nitrogen and cultured in an undifferentiated state in basal medium consisting of Dulbecco' s Modified Eagle' s Medium (DMEM; Biowest) supplemented with 10% fetal bovine serum (FBS; EuroClone), 100 u/mL penicillin (Biowest) and 100 u/mL streptomycin (Biowest). Once the cultures reached 70-80% confluence, the cells were trypsinized and plated for further passages, in order to expand the cultures. To induce osteogenic differentiation, DMEM was supplemented with 2% FBS, 50 µg/mL of ascorbate-2-phosphate (Sigma-Aldrich), 10^{-7} M dexamethasone (Sigma-Aldrich) and 10 mM of β-glycerophosphate (Sigma-Aldrich). Culture media was replaced every three days. Cells were maintained at 37°C in a humidified 5% CO_2 environment.

2.5.2 CELL CULTURE FOR RT-PCR

IN VITRO CULTURES OF PRIMARY MURINE MSCS

Mice were sacrificed by cervical dislocation before collecting tibias and femurs. Bone marrow cells were flushed and seeded in culture using MesenCult Basal Medium supplemented with 20% Mesenchymal Mouse Stimulatory Supplement (StemCell Technologies) and 1% Pen-Strept (Life Technologies)(Complete Medium). Cells were grown at 37°C in humidified atmosphere at 5% CO_2. Medium was changed every 3 days and cells were trypsinized at confluence and reseeded at $2x10^4$ cells/cm^2 (passage 1, p1). All experiments were performed at passage 2 (p2). Cellular density seeded onto the disks was $10^5/cm^2$. Cell count was performed at the undifferentiated state and after differentiation at 12 hours, 24 hours, 48 hours and 8 days. While the RT-PCR was performed at 0, 3 and 8 days. Viable and dead cells were evaluated by Trypan blue exclusion. This test is based on the principle that live cells possess intact cell membranes that exclude certain dyes, such as trypan blue, Eosin, or propidium, whereas dead cells do not.

All the experimental protocols on mice were conducted in compliance with DL 26/2014: implementation of European Directive 2010/63 on the protection of animals used for scientific purposes. All experimental protocols were approved by the Institutional Ethics Committee for Animal Use.

Reverse transcription to cDNA was performed directly from cultured cell lysate using the TaqMAN Gene Expression Cells-to-Ct Kit (Ambion Inc., Austin, TX, USA), following manufacturer's instructions. Briefly, cultured cells were lysed with lysis buffer and RNA released into this solution. Cell lysate were reverse transcribed to cDNA using the RT Enzyme Mix and appropriate RT buffer (Ambion Inc., Austin, TX, USA). Finally, the cDNA was amplified by real-time PCR using the included Taq- Man Gene Expression Master Mix and the specific assay designed for the investigated genes. Real-time PCR Expression was quantified using real-time RT-PCR. The gene expression levels were normalized to the expression of the housekeeping gene RPL13A and were expressed as fold changes relative to the expression of the untreated mMSC. Quantification was done with the delta/delta calculation method [24]. Forward and reverse primers and probes for the selected genes were designed using primer express software (Applied Biosystems, Foster City, CA, USA) and are listed in Table 3.

All PCR reactions were performed in a 20 ll volume using the ABI PRISM 7500 (Applied Biosystems, Foster City, CA, USA). Each reaction contained 10 ll 29 Taq- Man universal PCR master mix (Applied Biosystems, Foster City, CA, USA), 400 nM concentration of each primer and 200 nM of the probe, and cDNA. The amplification profile was initiated by 10-min incubation at 95 °C, followed by two-step amplification of 15 s at 95 °C and 60 s at 60 °C for 40 cycles. All experiments were performed including non-template controls to exclude reagents contamination. PCRs were performed with two biological replicates.

Table 3 Primers and probes used in real time PCR

Gene Symbol	Gene name	Primer sequence (5´ > 3´)	Probe sequence (5´ > 3´)
RUNX2	Runt-related transcription factor 2	F-TCTACCACCCCGCTGTCTTC R-TGGCAGTGTCATCATCTGAAATG	ACTGGGCTTCCTGCCATCACCGA
ALP	Alkaline Phosphatase	F-CCGTGGCAACTCTATCTTTGG R-CAGGCCCATTGCCATACAG	CCATGCTGAGTGACACAGACAAGAAGCC

2.6 STATISTICS

The measurements of the contact angle were repeated 3 times for each sample (n=3) calculating the angle created by 1µL H_20 and its surface. The mean value was calculated and a paired t-test was utilized to determine the differences in contact angle between the groups (Photofunctionalized discs and non-treated discs). A value of $P < 0.05$ was considered statistically significant.

MC3T3 and RT-PCR culture results are expressed as mean. Differences between experimental groups (Photofunctionalized discs and non-treated discs) were evaluated by Student's t-test. A value of $P < 0.05$ was considered statistically significant.

The chemo-physical studies were performed at the A. Chelkowski Institute of Physics, University of Silesia Katowice, Poland, at the Poland Silesian, Center for Education and Interdisciplinary Research, Chorzów, Poland and at the Refractory Materials Division, Institute of Ceramics and Building Materials, Gliwice, Poland . The biological studies instead, were performed at the Institute of Biomedical Technologies, National Research Council (CNR), Pisa, Italy and at the Dept. of Translational Research and New Technologies in Medicine and Surgery, University of Pisa Medical School, Pisa, Italy.

3. RESULTS

3.1. SURFACE ANALYSIS

Surface analysis on 2 different commercially available dental implants, osteoplant BASE and RAPID, was carried out to validate the theory that implant surfaces are covered with hydrocarbons and that this is not dependent on the manufacturers surface treatment. Therefore, initially we performed a thorough examination of the surface with various and complementary techniques, such as SEM, XPS, AES and AFM to determine a baseline result and then repeated after UVC irradiation of the implant surface. These analyses provided information on surface appearance, chemical composition and distribution, as well as roughness. Dental implants are considered unsuitable for biological experiments, because they do not have a flat surface that allow reliable cell evaluation. Therefore, titanium discs prepared with the same protocol of the implants were used for this purpose. However, before proceeding with the cell culture experiments, we performed on the discs the same chemo-physical tests employed to characterize the implant surfaces. Furthermore, we carried out an EDS analysis; to demonstrate the equivalence of the disc and implant surfaces.

3.1.1 XPS ANALYSIS:COMPOSITION OF IMPLANTS SURFACES

In Figure the XPS survey spectra of the reference BASE and RAPID implants are shown. The elements Ti, O, C, Al and F were detected. Titanium, oxygen and carbon were the main elements present on the implant surface, while aluminium and fluoride were deposited during the sand-blasting and acid etching procedures during manufacturing.

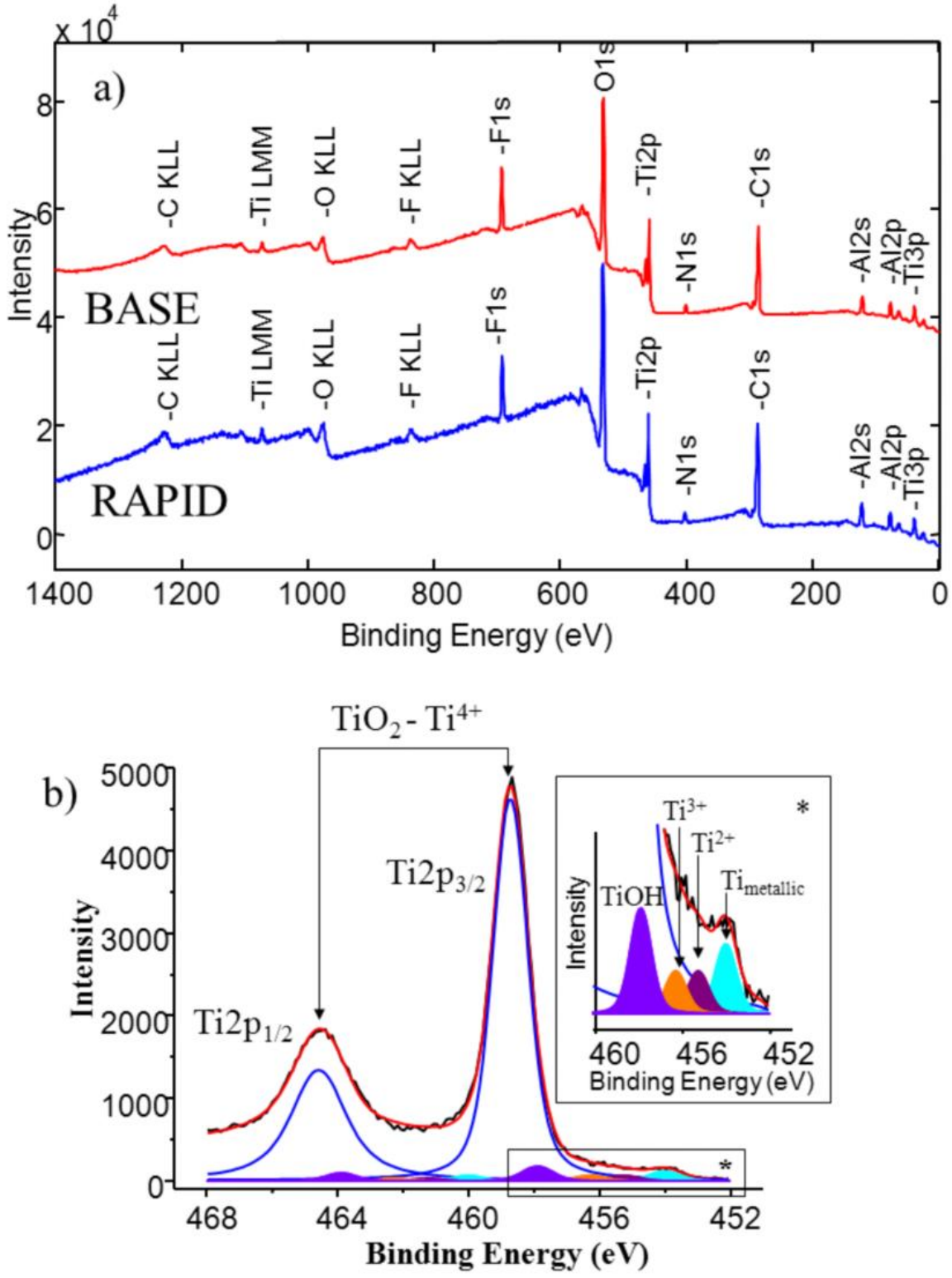

Figure 6 A) The XPS survey spectra obtained for the BASE (red) and RAPID blue) implants as received. On both surfaces Ti, O, C, Al, and F were detected. B) High resolution of the Ti2p core line for RAPID implant. The shape of the 2p doublet was fitted by five sub-doublets. The doublet with the highest intensity corresponded to TiO_2 component. The enlarged region presented the $Ti2p_{3/2}$ peaks corresponded to hydrated water Ti-OH, various oxidation states and metallic state of titanium

Table 5 shows atomic concentrations, obtained by XPS measurements, on the surface of both implant types. We found titanium (about 7% and 6% for the BASE and RAPID samples, respectively), oxygen (about 37%), aluminium (about 8%) and nitrogen (about 2%). The level of carbon contamination was about 39%.

Table 4 Atomic concentration of carbon, nitrogen, oxygen and titanium from C1s, N1s, O1, Al2p, Ti2p and F1s core lined for BASE and RAPID. The values reported in table have an error of Δ ± 0.1%

	Carbon	Nitrogen	Oxygen	Aluminum	Titanium	Fluoride
BASE	39 %	2 %	37 %	8 %	7 %	7 %
RAPID	39 %	2 %	38 %	8 %	6 %	7 %

The shape of the Ti2p doublet presented in Figure 6b consists of several components which can be ascribed to presence of Ti-OH bonds and various titanium oxides as reported by Kang [85]. The binding energy of the main peak of $Ti2p_{3/2}$ state at E=458.7 eV confirmed the presence of TiO_2 on the implant surface [86]. The metallic form of the titanium was also detected on the surface reference materials. We focused our study on the analysis of Ti, O and C. In Figures 7a and 7b the SEM images of the reference BASE and RAPID implants are shown. The distribution of different contrast from light to dark areas indicates a considerable degree of roughness of the analysed areas. The RMS value obtained from the AFM scan (Solver P47 NT-MDT instrument, non-contact mode) with size 15 x 15 μm was 0.4 μm. However, the

surfaces of both type implants are quite similar, as can be expected considering that both were sandblasted and acid-etched during manufacturing.

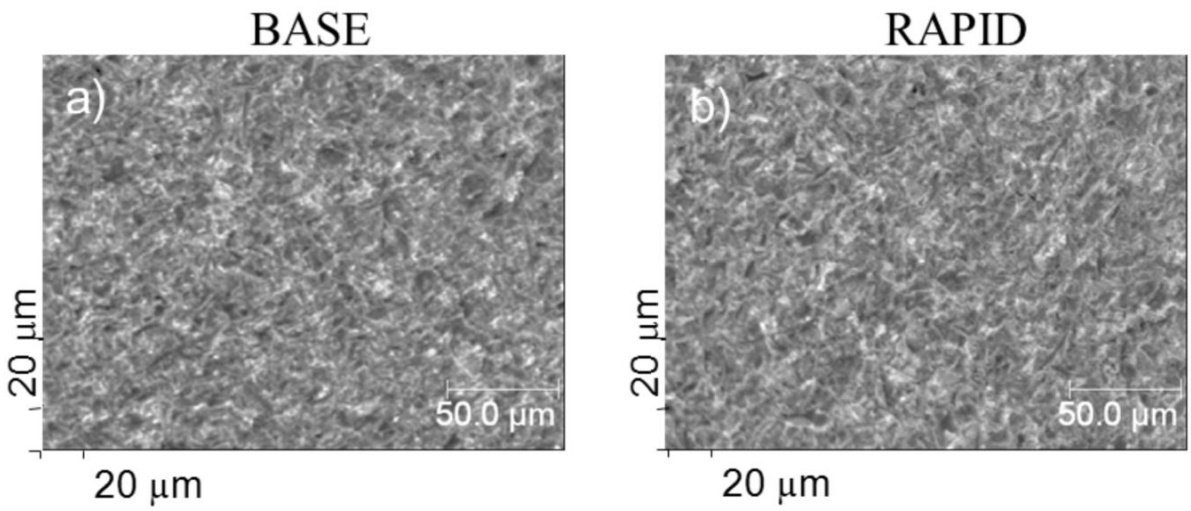

Figure 7 Electron microscope images obtained with magnification x500 recorded for BASE a) and RAPID b) implants as received. The contrast from light to dark areas suggest a considerable degree of roughness of the analysed area. Comparing (a and b) are similar in their topography.

The chemical distribution of carbon, titanium and oxygen has been shown in Figures 8a, 8b and 8c and presents a non-homogeneous grain type distribution for these elements on both implants. The carbon is spread all over the analysed area. Its atomic concentration in some parts achieves 63%. The oxygen is also very prominent on the surface. However, its maximum concentration of 38,6% is achieved only in a confined area. Distribution of titanium with respect to carbon and oxygen is almost homogeneous. However, its value of atomic concentration is very low. The presented results confirm the hypothesis that the implant surface is covered mainly by carbon and oxygen compounds.

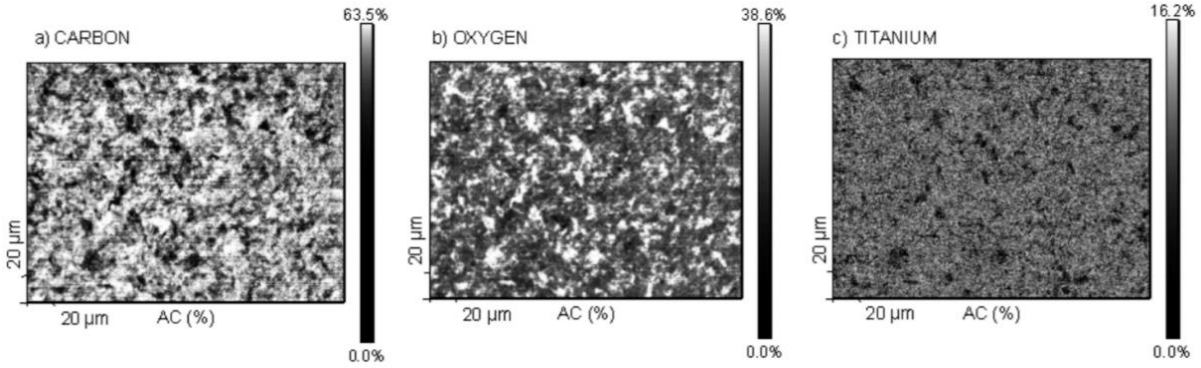

Figure 8 The chemical distribution maps of oxygen (a), carbon (b) and titanium (c) obtained for the RAPID implant. The distribution of the elements is grain type with carbon spread all over the surface while titanium is almost homogenous.

The present data shows that the outer layer of TiO_2 dental implants is covered by a layer of carbon atoms; during the manufacturing of the implants the surface is almost carbon free but with time it gets contaminated. This behaviour of titanium is defined as biological ageing. Our explanation is that the surface of freshly cut titanium is rapidly oxidized and consists of rows of bridging oxygen ions with 5 fold $Ti4^+$ ions (Ti5c), in plane oxygen, fully coordinate titanium (Ti6c) and O-vacancies defined as defects. This composition can be stable only if kept in the UHV (Ultra High Vacuum), if exposed to the atmosphere the unsaturated Ti5c atoms form bonds with H_2O molecules forming therefore, hydroxyl groups (-OH). This coverage is the reason for the hydrophilic character of fresh titanium, however the surface still is not completely stable and continues to form bonds also with hydrocarbons, explaining why there is a high presence of both oxygen and carbon on implants which are older than five weeks.

In order to distinguish the type of carbon and oxygen contamination and to verify the effectiveness of UVC in decontaminating titanium surfaces, the core lines O1s and C1s were recorded for the RAPID and BASE implants before and after treatment. Because the analysis of the RAPID and BASE gave the same results (table 5) from now on only the results for the RAPID material will be presented. In Figure 9a and 9b we present results of C1s and O1s measurements obtained for the implant as received and after photofunctionalization.

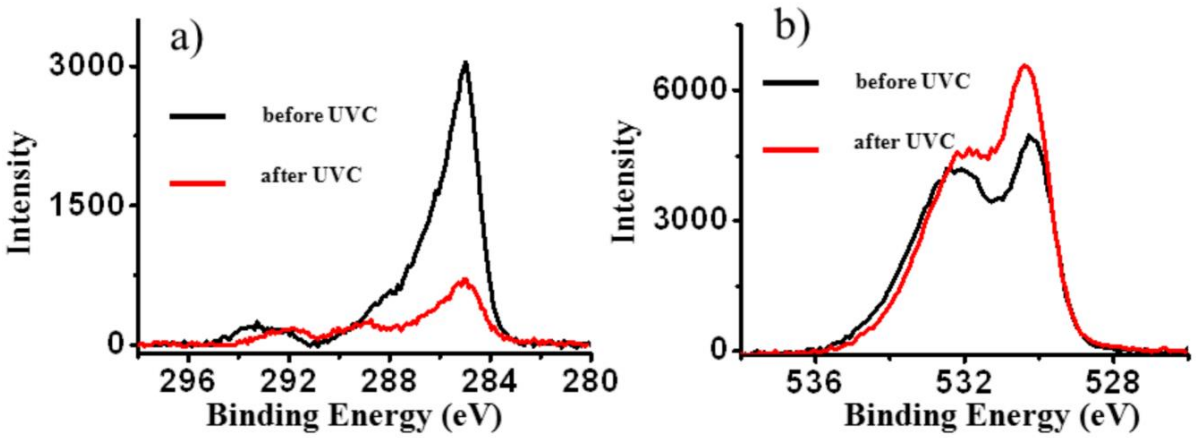

Figure 9 The C1s (a) and O1s (b) core lines recorded for as received and after photofunctionalization samples. The lines in red show the decontamination effect of the UVC irradiation decreasing the hydrocarbons peak and increasing the Oxygen peak

Remarkably we observed a drastic decrease of carbon after UVC irradiation figure 9a. In contrast the signal of oxygen resulted in a small increase of signal figure 9b. Additionally, the shape of both measured lines is combined with additional components. The results of the deconvolution of the experimental lines is presented in Figures 10a–d.

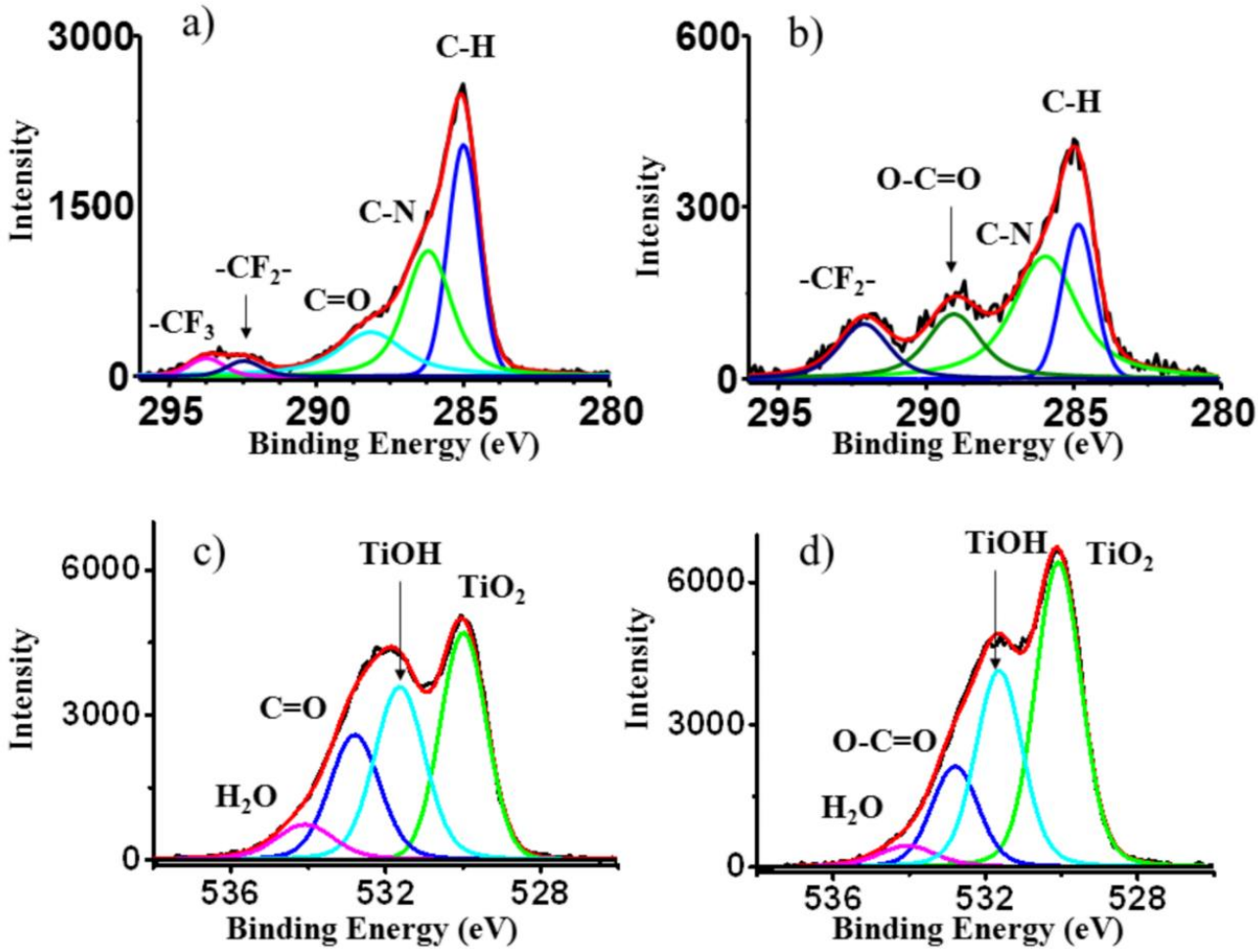

Figure 10 Line shape of C1s and O1s spectra for the implant as received (a and c) and after photofunctionalization (b and d). Comparing (a and b) the intensity of the peak at 285 eV corresponding to the carbon contamination is highly reduced. The oxygen lines (c and d) show an increase in oxygen peak.

The C1s spectral profile in Figure 10a consists of five components. The component with the highest intensity at energy E=285 eV corresponds to the C of hydrocarbons. The second component corresponds to the C-N chemical group, and the third to the CO group of molecules present on the surface. The last two components with the highest binding energy can be ascribed to the presence of $–CF_3$ and $–CF_2$ groups. The analysis of the O1s core lines is reported

in Figure 10c. The O1s line shape consists of four components. The component with the highest intensity corresponds to TiO_2, the second corresponds to TiOH groups, the next component can be ascribed to C=O groups and the last one corresponds to H_2O linked to surface Ti atoms. The changes in intensity of C1s and O1s spectra after UVC irradiation are reported in Figures 10b and 10d, respectively. The intensity of all four components for carbon, corresponding to C-H, C-N, O-C=O and $–CF_2$- bonding, drastically decreased. In the case of the O1s spectrum the signal corresponding to oxygen atoms of TiO_2 slightly increased. The peak at 534 eV corresponds to H_2O molecules present on TiO_2. Comparing its intensity before and after UVC irradiation a slight decrease was observed. On the other hand, a minor increase in the intensity of TiOH was observed while, that of carbon dioxide was slightly decreased.

The results of atomic concentration calculations for C, O and Ti obtained by XPS and AES methods before and after photofunctionalization are presented in Table 6. In the case of N only the XPS value is given, because in AES the peak corresponding to nitrogen (N KLL) overlaps the peak of Titanium (LMM), therefore the N component is impossible to distinguish. Hence, the Ti LMV Auger peak was used for AES calculation of atomic concentration. The values of the atomic concentrations calculated for the RAPID implant as received from the AES and XPS data were almost the same, confirming the equivalence of the two methods. The atomic concentration of C decreased by about four times, while in the case of O and Ti an increase of atomic concentration was observed. The amount of N decreased by about 1%.

Table 5 Atomic concentration calculations obtained from the AES and XPS spectra for the surfaces of RAPID implant as received and after UVC irradiation.

	Carbon	Nitrogen*	Oxygen	Titanium
AES/XPS ***Before irradiation***	47/43	2	45/47	8/8
AES/XPS ***UVC 12 min cycle***	13/14	1	75/69	11/13

value recorded only with XPS

3.2.2BIOLOGICAL AGEING

In figure 11 the changes of the ratios of carbon and oxygen to titanium during the period 10 weeks have been shown. The strong decreasing of carbon contamination is visible after UVC treatment. On the TiO_2 discs the amount of carbon in ratio to Ti decreased about three times. Exposure to the atmosphere of the samples surface led to a logarithmic increase of the amount of carbon within 10 weeks. It is interesting that after 6 weeks the contamination by carbon pollution reaches the initial level and it is even increasing. The influence of UVC treatment led to a rapidly decrease of the O/Ti ratio. During the first 4 weeks the oxygen level is rapidly increasing while after the this period it stabilizes.

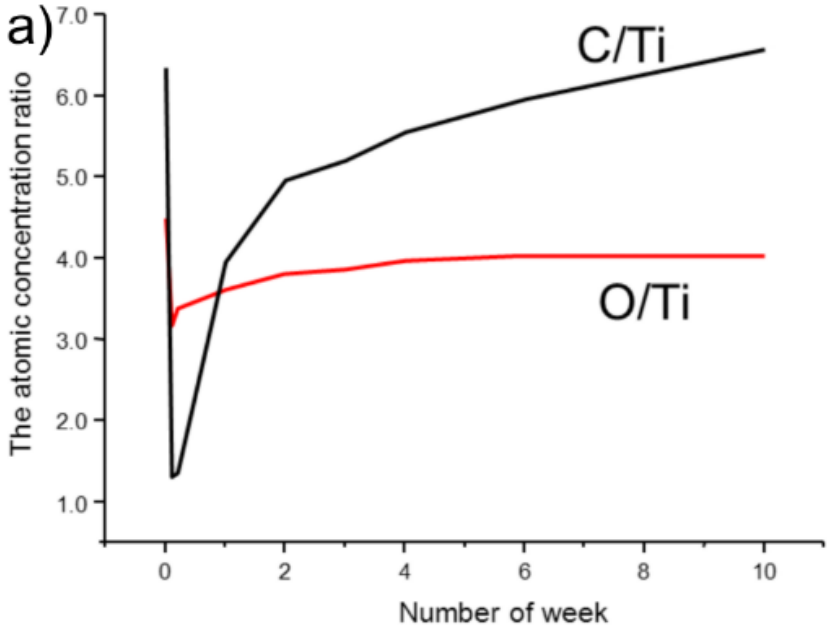

Figure 11 Biological ageing

3.2.3 XPS OF TITANIUM DISCS

As previously mentioned the same type of chemical analysis performed for the dental implants it has been repeated for titanium discs. This was necessary to determine that the baseline which allow biological assay for cells seeded onto titanium surface considering that on a dental implant would not be possible. Figure 12, shows the difference in survey spectra before and after UVC irradiation. As for the implants here below are presented the data concerning sand-blasted/ acid etched grade 4 discs because no difference was found between the different surfaces. During the analysis carbon, oxygen, fluoride, aluminium and titanium. Of our interest is the peak present at 285 eV corresponding to C1s greatly decreases in intensity after UVC irradiation in agreement with the results in Table 7. The atomic concentration of the elements detected from the XPS of the titanium disks are similar to the results obtained for the implants in the section discussed earlier (table 6 and 7). The level of C1s detected on the disk before and after UVC irradiation was 33,2% and 16,2% respectively. Instead the signal for O1s detected an increase from 46,2% before irradiation to 58,1% after irradiation.

Table 6 XPS analysis of the titanium disks comparing the difference in chemical composition before and after 12 minutes UVC irradiation. The values reported in the table have an error of Δ ± 0.1

	C1s	O1s	F1s	Al2p	Ti2p
XPS Before UVC irradiation	33.2	46.2	4.7	8.1	7.75
XPS After UVC irradiation	16.2	58.1	4.1	10	11.6

a)

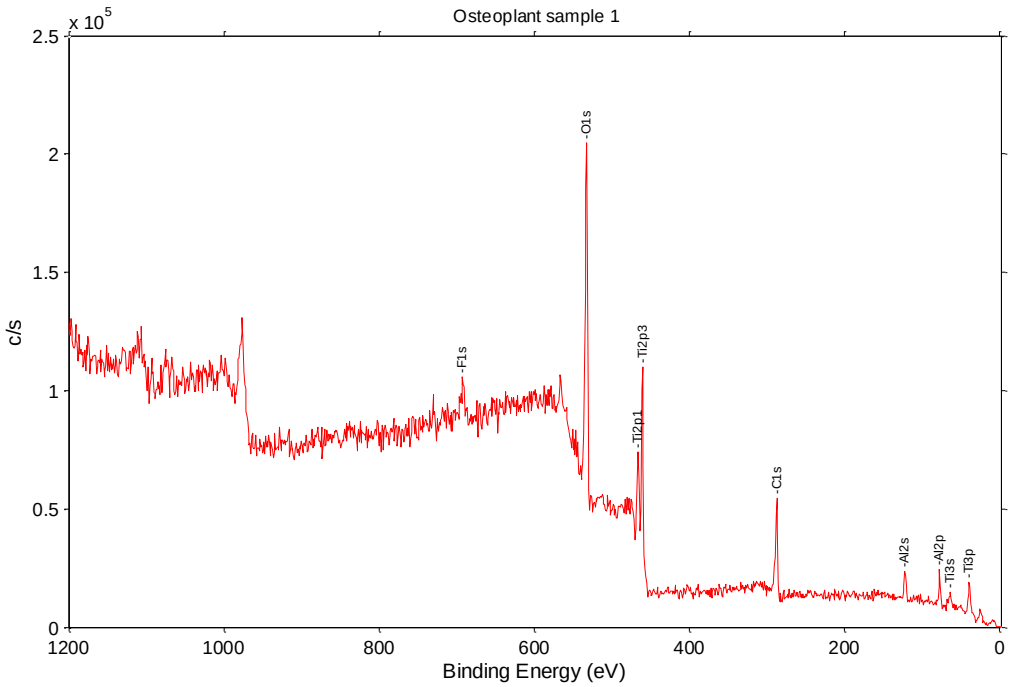

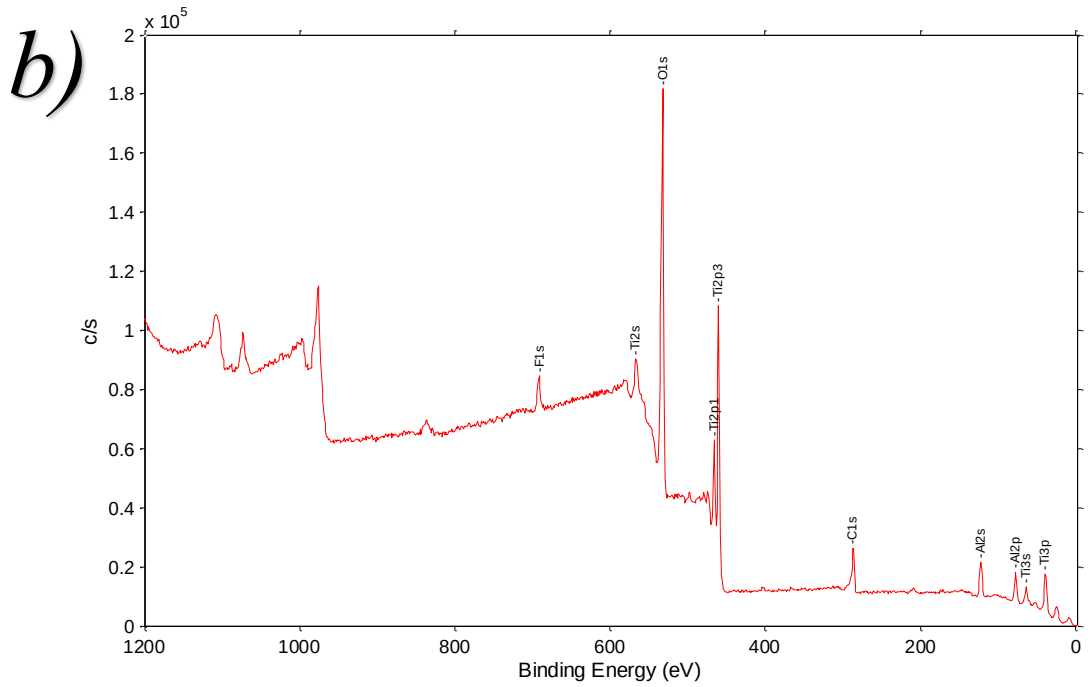

Figure 12 XPS Spectra of titanium disc. A) before UVC irradiation B) after UVC irradiation

3.3 EDS: ATOMIC MAPPING OF THE ATOMS ON TITANIUM DISC

The study of microstructures performed by secondary electron detector (SE) shows a compact surface with high roughness with feather sharp shaped grains. The photographs obtained by backscattering electrons detector (BSE) indicates the existence of two uniform phases on the surface FIGURE 13 A . The results of the elemental distribution measurements in micro-areas obtained by Energy Dispersive X-ray Spectrometry (EDS) indicate dominant chemical composition of Ti indicated as light blue spots (Fig 14 b5), Al, indicated as blue spots (Fig 13 b4) and O ,indicated as red spots(Figure 13 b2), on the surface. The presence of other elements like fluoride, indicated as yellow spots (fig 13 b3), is probably due to remnants of the etching procedure during manufacturing. Aluminum detected on the disc surface (fig 13b 4) is partly due to the chemical composition of the implant alloy (Ti-6Al-4V) and also due to the residues derived from the sand-blasting process. The EDS data are in agreement with the AES and XPS results previously described. The mutual arrangement of all elements suggests that the sample

is composed mainly of titanium, with BSE detector it corresponds to the brighter surface in fig 13a , and aluminum oxide, which corresponds to the darker area. Interestingly, the distribution of Oxygen (red spots Fig 13 b2) and the one of carbon (purple spots fig 13 b1) looks very similar. That is because the hydrocarbon have a carboxylic group (COO^-) which fits perfectly between the titanium atoms and bridging oxygen of the Ti5c.

A

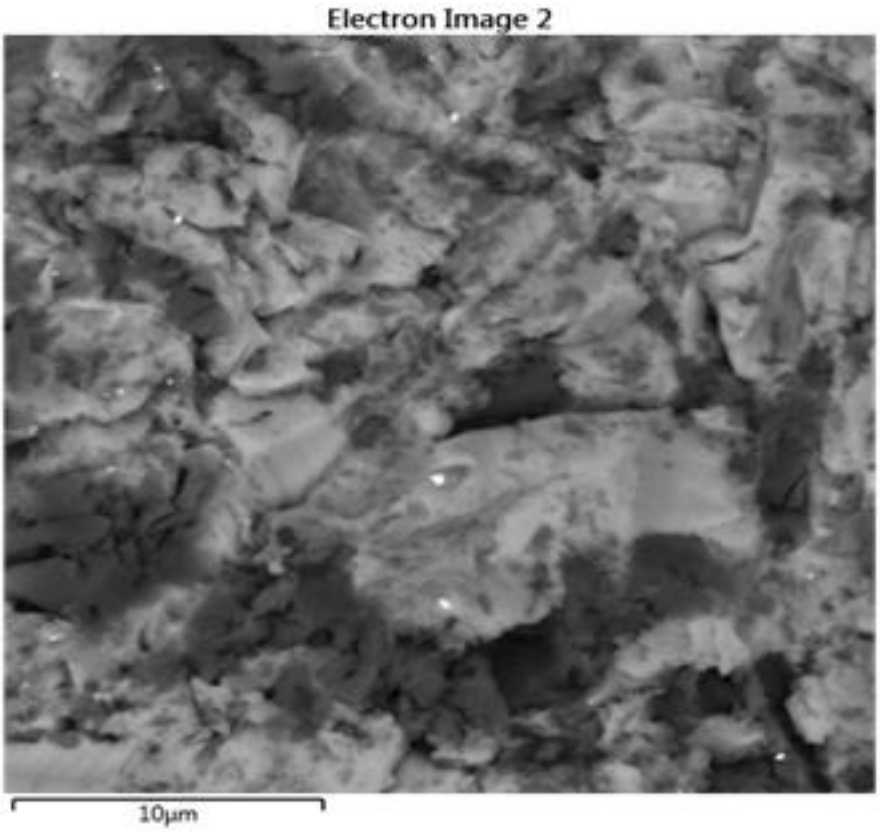

x1000

B EDS map

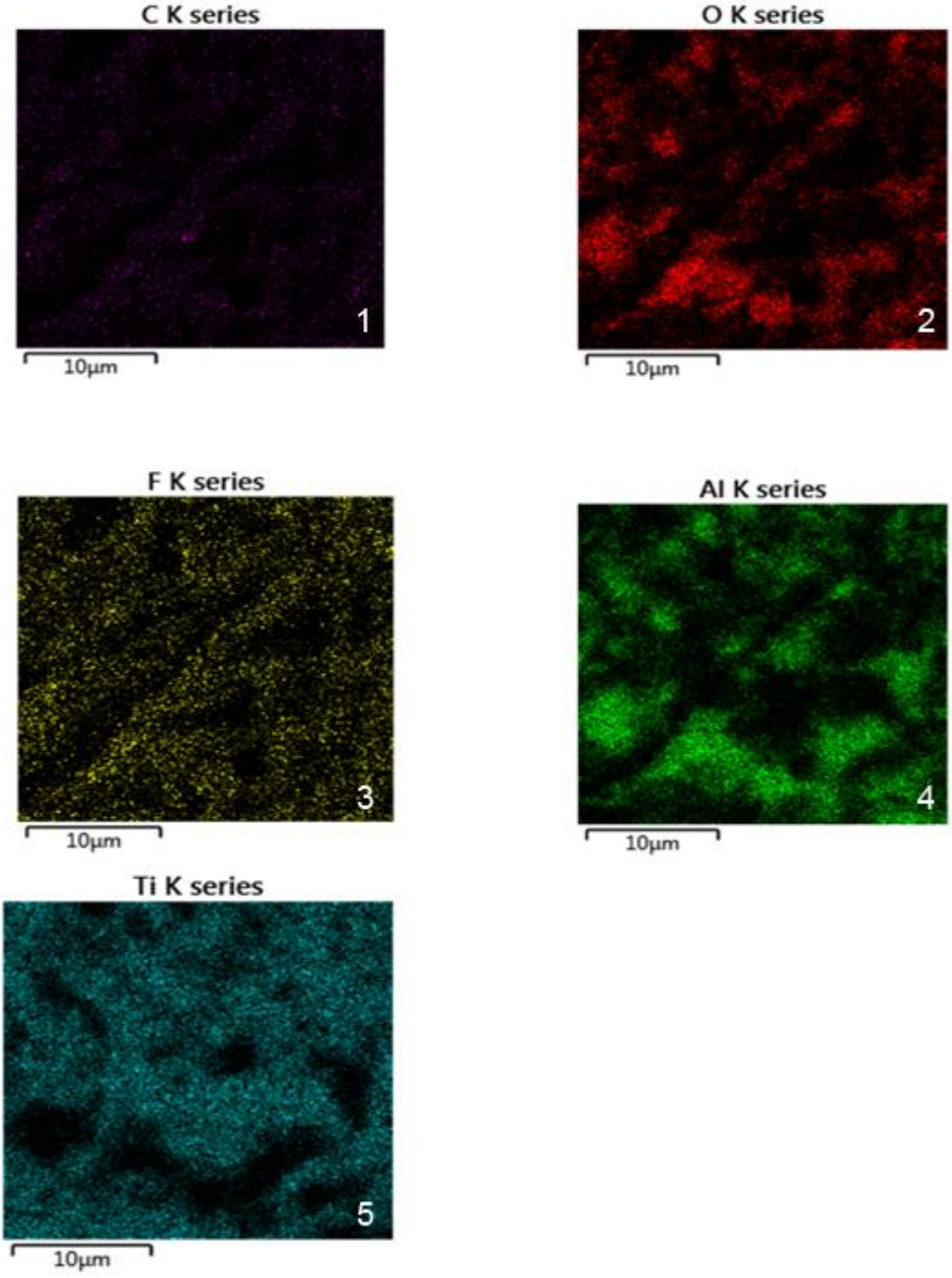

Figure 13 a) SEM image of the analysed area b) Distribution of the atomic concentration obtained at the magnification x1000 for the C (b1),O (b2), F (b3), Al (b4) and Ti (b5) elements of the sample disc before UVC irradiation

3.4 AFM ANALYSIS FOR DETERMINATION OF ROUGHNESS

The atomic force microscopy is an invaluable test to measure small samples with a great degree of accuracy. It is imperative to use this analysis to demonstrate that the UVC treatment does not change the topography of the surface after the company manufacturing. The analysis was performed for the dental implant Osteoplant Rapid and the titanium disks. It was important to compare the topography between the different samples to understand their similarities.

3.4.1 AFM OF THE IMPLANT

In figure 14 a typical image with relatively large scanned area 15 x 15 μm of flat part of implants screw is presented. It contains a number of valleys and hills of height about 2 μm with relatively rough surface. The typical coefficient of rough mean square (RMS) was about 0.4 μm. The area of analysis was slightly lower when compared to the discs samples because to have precise measurements the surface signal of the AFM needs to be directed perpendicular to the surface. Thus, we set the experiment to set up optimal conditions and the area 15 x 15 (μm) was judged to be the most reliable.

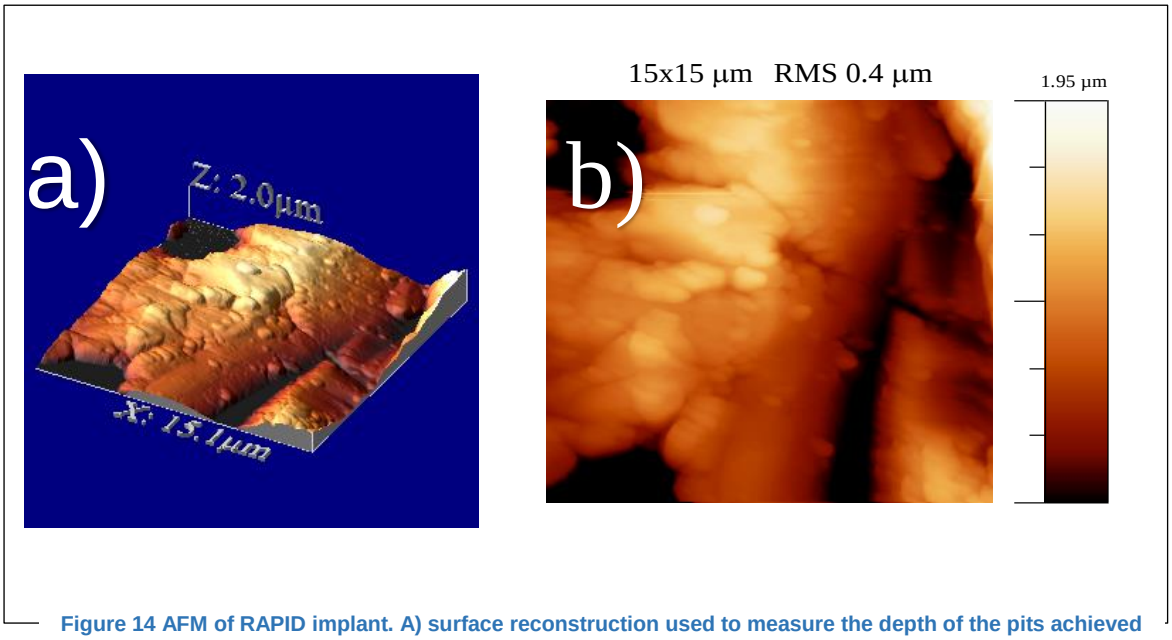

Figure 14 AFM of RAPID implant. A) surface reconstruction used to measure the depth of the pits achieved during the manufacturing processing. B) Magnification of an area of the implant with size 15 x 15 *μm* to calculate the RMS value.

3.4.2 AFM OF THE DISCS

Surface roughness plays a significant role on cell behaviour during the process of osteointegration. The XPS and AES analysis demonstrated that the surface composition of the discs is the same as the one of dental implants, however they could not give any information regarding the surface roughness. Therefore, AFM analysis was necessary to indicate if the discs which were going to be used during the biological studies have the same surface roughness of dental implants.

Surface analysis performed by atomic force microscopy method (AFM) worked in non-contact mode. In this mode the cantilever vibrates under the surface with fixed frequency. The images of topography are created as the results of measurements of the offset from the resonance frequency of cantilever during the effect with the surface. In figure 15 is presented the topography images of the machined titanium discs with area of 50x50 µm and about 20x20 µm for sand blasted/acid etched grade 2 and grade 4, respectively. Before the analysis the samples were cleaned in isopropanol medium in ultrasonic washer. In figure 15 (A) the machined sample presents the grooves and small particles characteristic of the machining process. The smaller area (20 x 20 micrometers) shows valleys and numerous depressions. The calculated rough mean square RMS coefficient is 0.30 µm ±0.01 and 0.12 µm ± 0.01, respectively.

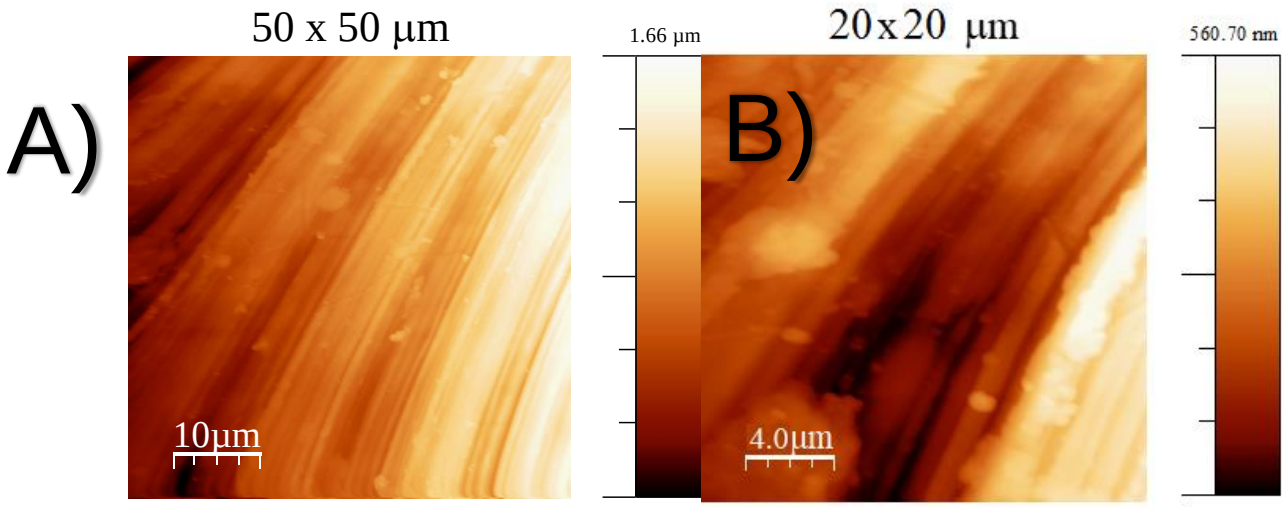

Figure 15 AFM analysis of machined titanium discs for 2 different area. A) area of magnification 50x50 µm B) area of magnification 20x20 µm

The topography of surfaces after sand-blasting and acid etching look very similar independently of the grade of titanium Fig 16. Both samples exhibit granular structure with similar maximum heights of about 2 µm for the 50 x 50 area and about 1.5 µm for the area of 20 x 20 µm. Both samples present numerous holes. The RMS coefficient was 0.38 ± 0.01 and 0.46 ± 0.01 µm for the recorded area 50 x 50 µm and 0.25 ± 0.01 and 0.30 ± 0.01 µm for the area 20 x 20 µm obtained for the sand-blasted/acid etched grade 2 and sandblasted/acid etched grade 4 surface, respectively Table 8. The RMS coefficient is higher for sand-blasted/ acid etched grade 4 than the machined and sand-blasted/ acid etched grade 2 surface. Hence, we concluded that grade 4 sandblasted/acid etched modification had the highest roughness coefficient and overall the samples had similar characteristics as the implants used in the first part of the study. The test was repeated after UVC irradiation and no changes were detected. It suggests that UVC does not alter the surface topography

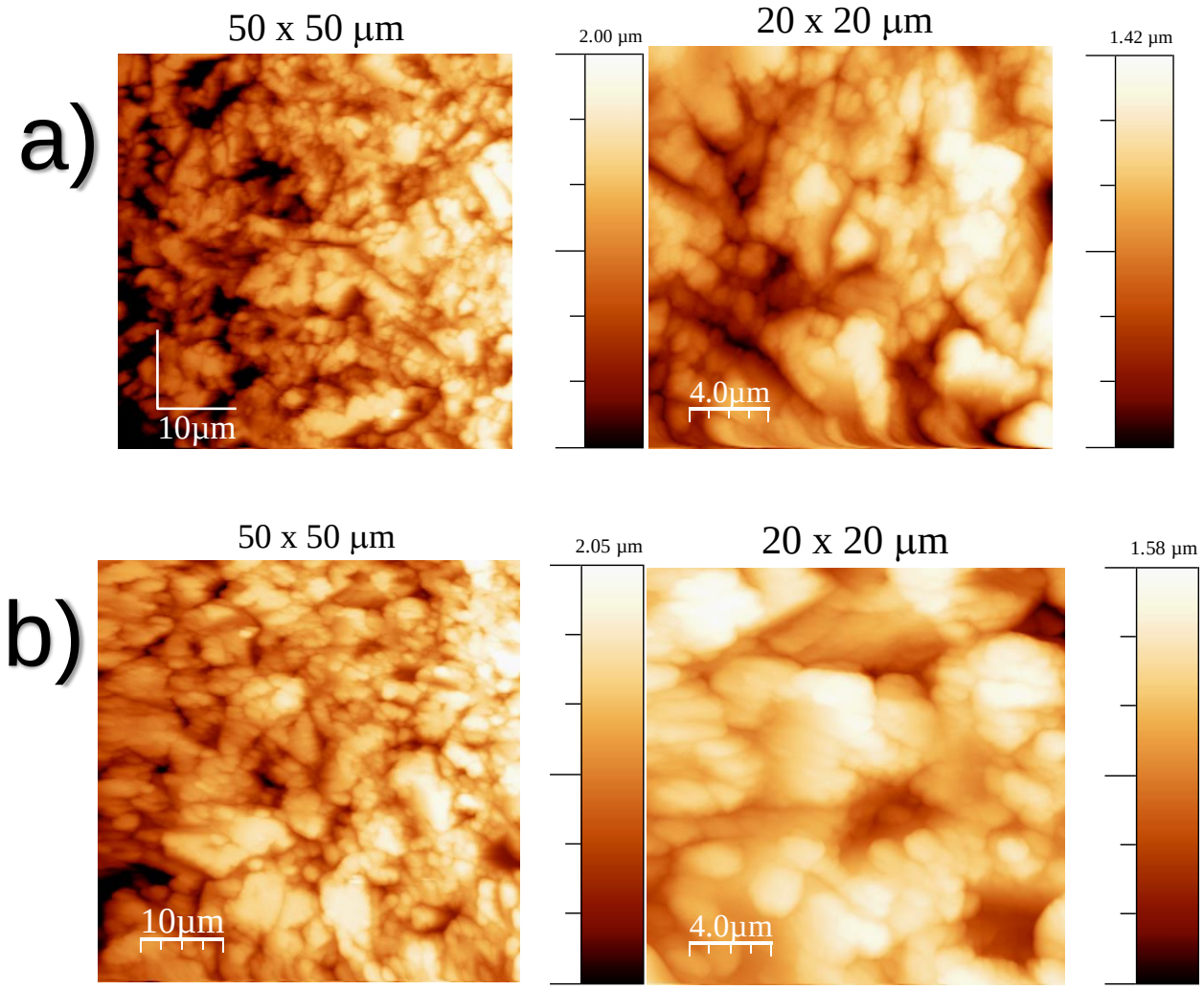

Figure 16 Comparison of AFM analysis of sand-blasted / acid etched discs. a) Sandblasted/ acid etched grade 2 b) sandblasted/ acid etched grade 4

The AFM scanning results (TABLE 8) showed the sand blasted/acid etched surfaces exhibited higher roughness values as compared with the machined surfaces.

Table 7 Roughness values Ra µm for each sample in different surface area.

Area	Machined surface (μm)	Sand-blasted acid etched grade 2 (μm)	Sand-blasted acid etched grade 4 (μm)	Dental implant (RAPID) (μm)
50x50 μm	0.30	0.38	0.46	-
20x20 μm	0.12	0.25	0.30	-
15X15 μm	-	-	-	0.4

*The values reported in the table have an error of ± 0.01 µm

3.5 CONTACT ANGLE / WETTABILITY

Cell attachment is strongly dependent on the surface energy, which is described as surface wettability. The test utilized to study this parameter is the contact angle; which indicates that if it has a low value means that the surface is hydrophilic while an high value means that the surface is hydrophobic. The fluid medium used for the contact angle measurement must meet several requirements: (1) low viscous, (2) low specific weight, and (3) chemically inactive against the substrate surface. To evaluate contact angle we use (or deionized) water is normally employed in literature, as it meets the requirements for a reliable measure. After UVC exposure (12min) the contact angle measurements of distilled H_2O droplet was measured for 3 different surfaces, machined surface grade 2, sand-blasted/ acid etched grade 2 and grade 4.

Then the samples were stored at atmospheric conditions for 4 weeks. The results are illustrated in the graph below Figure 15.

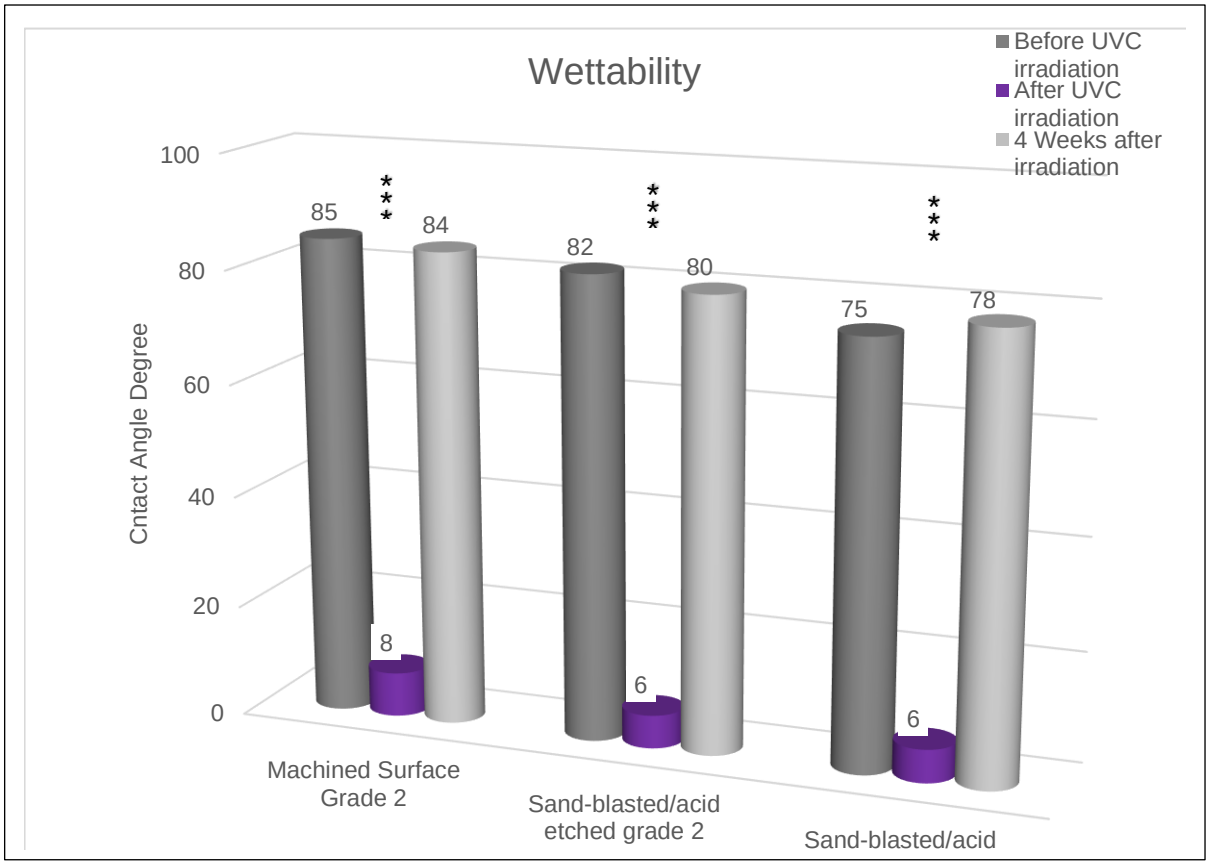

Figure 17 Surface contact angle before UVC irradiation, immediately after UVC irradiation and after 4 weeks of storage in the air. Machined Grade 2, Sand-blasted/acid etched grade 2, Sand-blasted/ acid etched grade 4 are respectively represented. Dark grey values represent the contact angle of the disk before irradiation, the purple line immediately after UVC irradiation and the light grey indicates the same surface after 4 weeks of atmospheric storage. Results were performed in triplicate and are shown as the mean, all the values recorded were within ± 0.5 ° of the mean . For statistical analysis the contact angle obtanied for the photofunctionalized discs was compared to the non- treated, used as control. *P < 0.05; P < 0.01; P < 0.001

Machined surface had an average contact angle of 85 °, after UVC irradiation the value decreased to 8° Fig 18 and after 4 weeks of storage the contact angle increased to its initial level. Both the sand-blasted/acid etched grade 2 and grade 4 surfaces started from a lower

contact angle value 82° and 75° respectively. After UVC irradiation the contact angle decreased to 6° for both of the surfaces. As for the machined surface after 4 weeks of atmospheric storage the initial contact angle was restored Figure 17.

Comparing the machined surface to the sand blasted/ acid etched it can be established that UVC irradiation produced a highly hydrophilic status independently of the roughness and surface treatment (Figure 17).

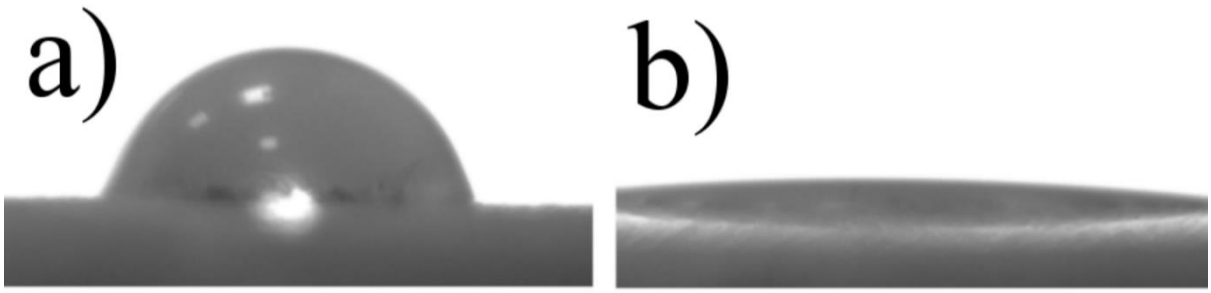

Figure 18 Photographic image of cantact angle measurament of 1 *µL* H_2O droplet. A) non-treated TiO_2 machined disc, contact angle 85° (hydrophobic) b) same disc after UVC irradiatin, contact angle 8° (super hydrophilic)

3.6 BIOLOGICAL EFFECTS OF UVC TREATMENT ON OSTEOGENIC CELLS

As primary MSCs represent a rather heterogeneous cell population, initial biological studies were carried out using a cell line MC3T3-E1, frequently used as an vitro model of osteogenesis.

The MC3T3-E1 cell line, derived from rat calvaria, has provided a useful means for optimizing methodological aspects and initial analysis of gene expression, as it is a non-transformed cell line and represents a relatively homogeneous cell population at a specific stage of differentiation, containing mostly pre-osteoblastic cells. Moreover, these cells can be induced to differentiate into mature osteoblasts. Therefore, cells were grown *in vitro* and maintained in expansion conditions or induced to osteogenic differentiation following exposure to specific osteogenic agents. As a first step, we evaluated cell survival/proliferation of the pre-osteoblastic cell line seeded onto 3 different TiO_2 surfaces, before and after UVC irradiation. We compared grade 2 titanium disks exposed to machine or sand-blasted Acid etched treatment, as well as grade 4 sand-blasted Acid etched titanium disks. The latter ones are more similar to the surface of the dental implants used clinically and equivalent to the implants used during the chemo- physical studies reported in previous sections.

Cells were counted 24 hours after seeding, as the initial attachment and proliferation of the cells is considered crucial to achieve a successful osteointegration. Results, illustrated in fig. 18, show that in all disks the number of living cells after photofunctionalization is highly significantly ($P < 0.001$) increased than the number of cells counted on untreated disks. The data, shown as a ratio between living cells measured in treated and non treated disks, indicate a 2.5, 1.8 and 2.8 fold increase of live cells in Gr2 machined disks, Gr2 sand blasted acid etched disks and Gr4 sand blasted acid etched disks, respectively, after UVC treatment. By trypan blue exclusion, we also evaluated the percentage of dead cells, which, following photofunctionalization, were virtually absent in Gr2 machined disks, but equally present as viable cells in UVC treated Gr2 sand blasted acid etched disks (Fig. 19 a). Fig 19 b shows an example of the results obtained in grade 2 sand-blasted Acid etched titanium disks, where an increased number of live cells can be observed in photofunctionalized disks.

Photofunctionalization of Gr4 sand blasted acid etched disks resulted in a two third reduction of dead cells, as compared to their frequency in untreated disks (Fig 19c). We also analysed the cells with a fluorescent microscope, after staining the cells nuclei Hoechst dye.

a)

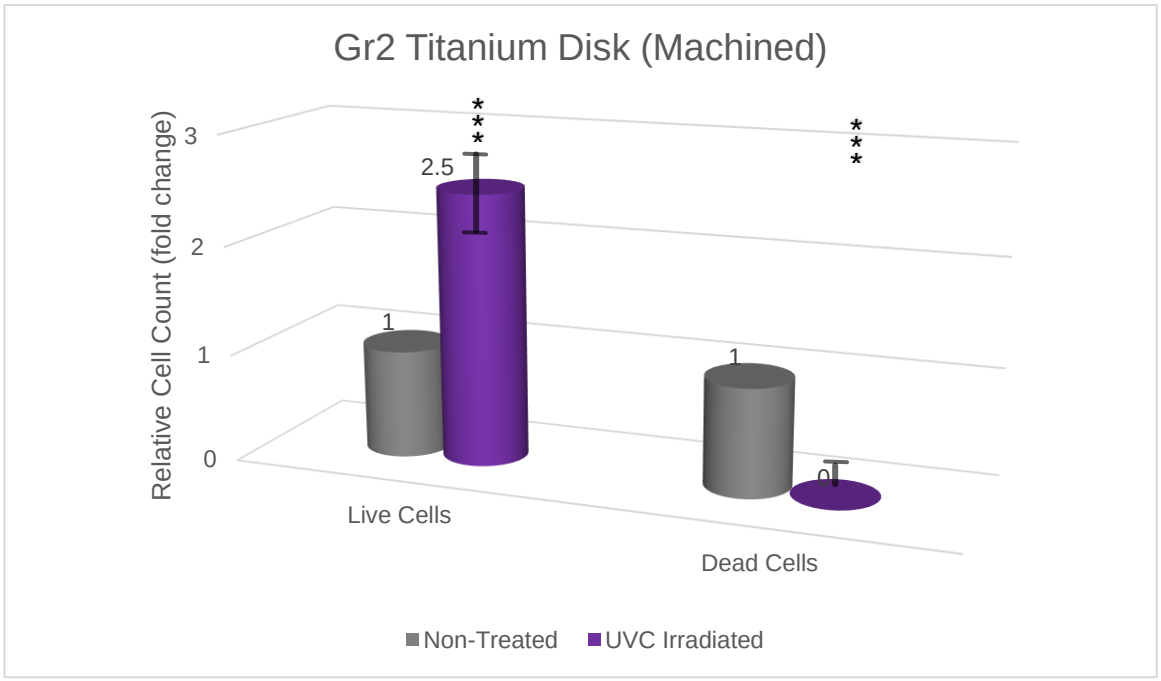

b)

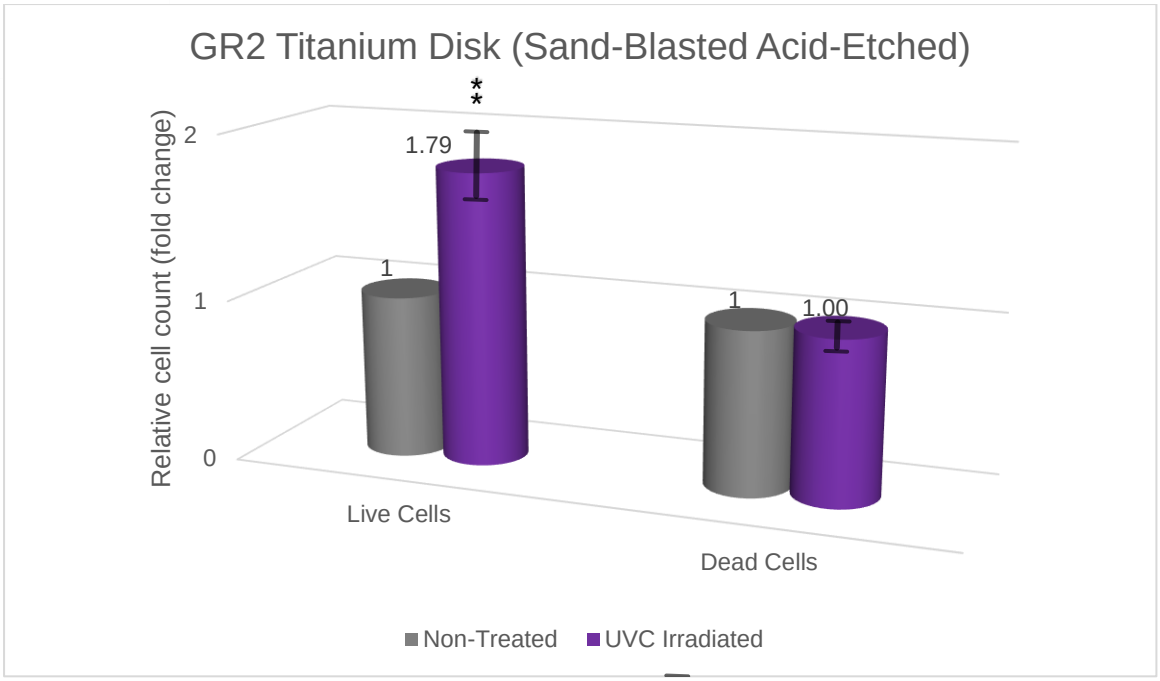

c)

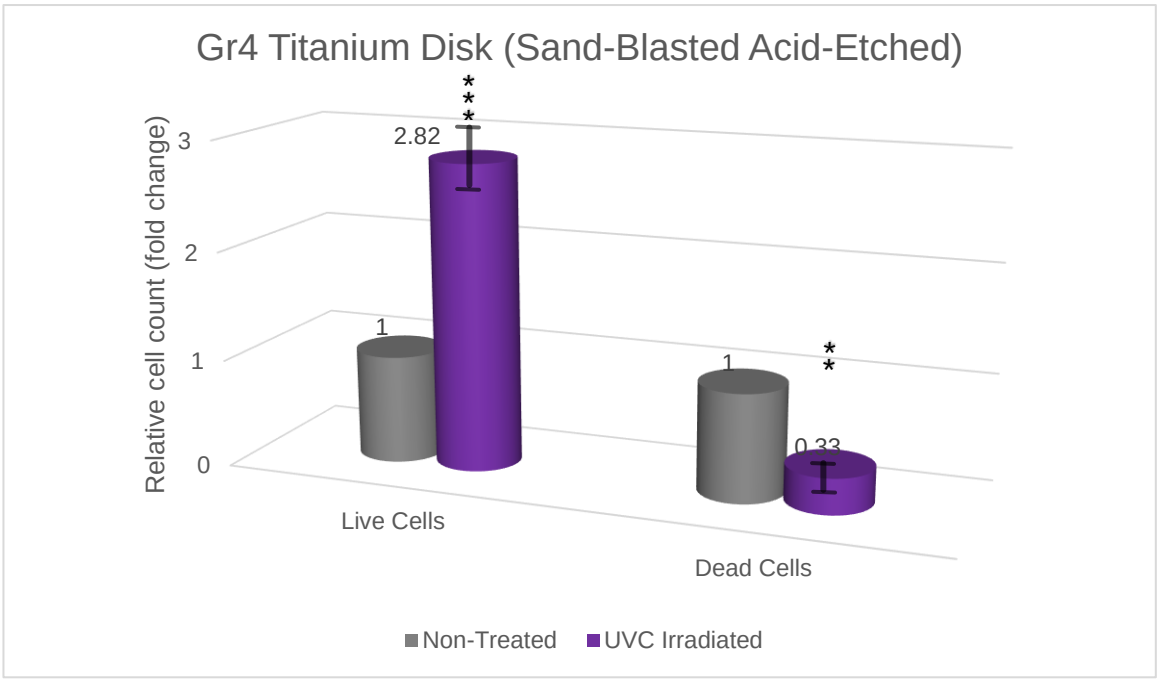

Figure 19 Attachment/proliferation MC3T3 after 24 hours a) results for titanium grade 2 surface machined b) results for titanium grade 2 sand-blasted/ acid etched c) results for grade 4 sand-blasted/ acid etched. Results were performed in triplicate and are shown as the mean. For statistical analysis the cell count obtained for the photofunctionalized discs was compared to the non- treated, used as control. *P < 0.05; **P<0.01; ***P<0.001

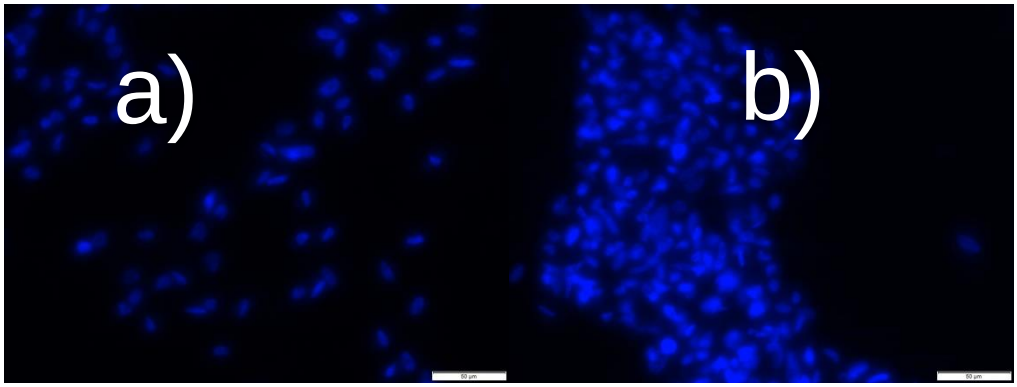

Figure 20 Fluorescence of MC3T3 staining of the cell nuclei with Hoechst dye, after 24 hours seeding on grade 4 sand-blasted/ acid etched surface.

As a second step we moved to study the effects of UVC treatment on primary MSCs, derived from murine bone marrow, cultured either in expansion conditions or at different time intervals after osteogenic induction. The choice of analyzing early times after osteogenic treatment is based on previous studies by Picchi et al, where the osteogenic process has been thoroughly monitored, which highlighted that the molecular events orchestrating osteogenic commitment take place shortly after osteogenic induction[87].

As in the experiments previously described on the pre-osteoblastic cell line, we first compared the percentage of viable cells in Gr4 sand blasted acid etched disks, before and after photofunctionalization. Fig 21 shows that, consistently with the data obtained using MC3T3 cells, 24 hours after seeding, the number of viable primary MSCs counted on non photofunctionalized disks was half the number of cells grown onto photofunctionalized disks. Moreover, following osteogenic induction, we observed a progressive and dramatic decrease of living cells in non photofunctionalized disks, as compared to cells seeded onto UVC treated disks. At 8 days of osteogenic differentiation, the cells present on untreated disks were only a very small percentage (around 4%) of the cells grown on irradiated surfaces.

We next analysed the expression of two osteogenic markers, Runx2 and ALP, at 3 and 8 days after osteogenic induction. As previously pointed out, Runx2 is the master gene of osteogenesis and Fig 22 shows that at 3 days of differentiation its transcriptional activity is up-regulated (doubled) in cells grown onto photofunctionalized disks, as compared to undifferentiated cells. However this increase has not been detected in cells cultured onto non-functionalized disks. As a further control, the same analysis was carried out in MSCs grown and differentiated in classical culture conditions, namely in plastic dishes. Also control cells show a 3 fold increase of Runx2 expression after 3 days of osteogenic differentiation. In addition, our results show that the transcriptional activity of the enzyme ALP is augmented in cells grown on all surfaces.

Similar, and more clear-cut findings were observed after 8 days of osteogenic induction, when the mRNA levels of both Runx 2 and ALP were significantly increased only in cells seeded onto Photofunctionalized disks ($P < 0.001$). Fig. 23 In contrast, virtually no variation was detected in the expression of both markers in MSCs grown onto non irradiated disks.

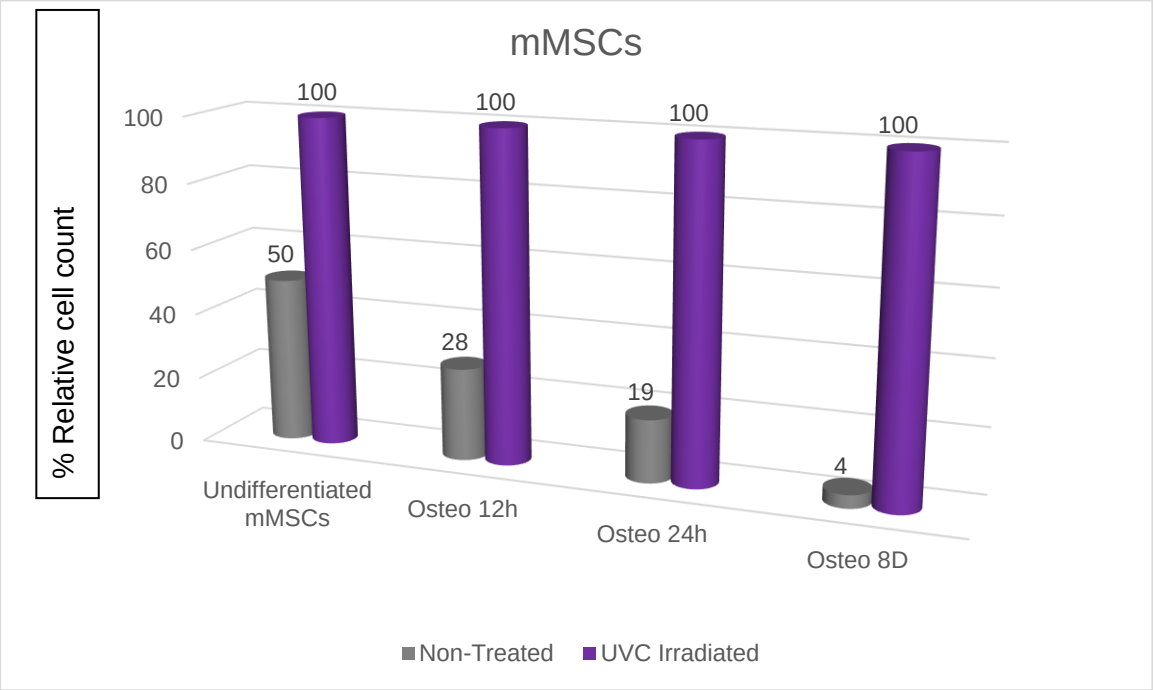

Figure 21 Cell attachment/ proliferation of Mmsc cells before differentiation and after differentiation to osteoblasts at 12 hours, 24 hours and after 8 days.

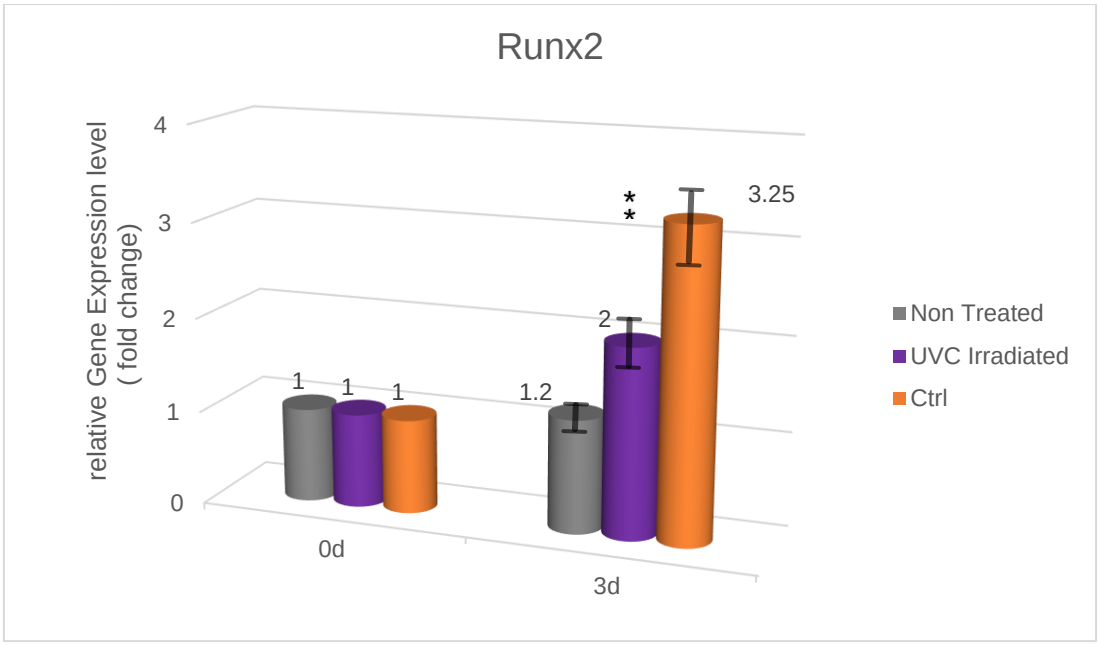

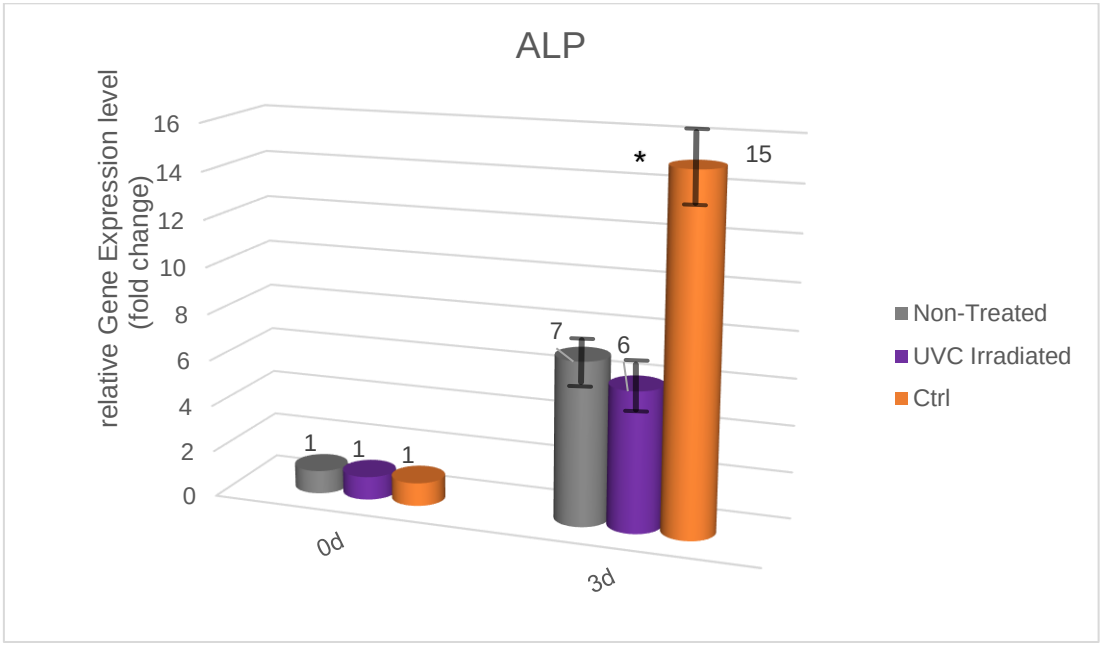

Figure 22 RT-PCR of the transcription factors RUNX2 and ALP of the undifferentiated mMSC and at 3 days after proliferation. Results obtanied in triplicate are shown as the mean. For statistical analysis RT-PCR results obtanied for the photofunctionalized discs was compared to the non- treated and with no disc used as control. *P < 0.05; ** P < 0.01; *** P <0 .001

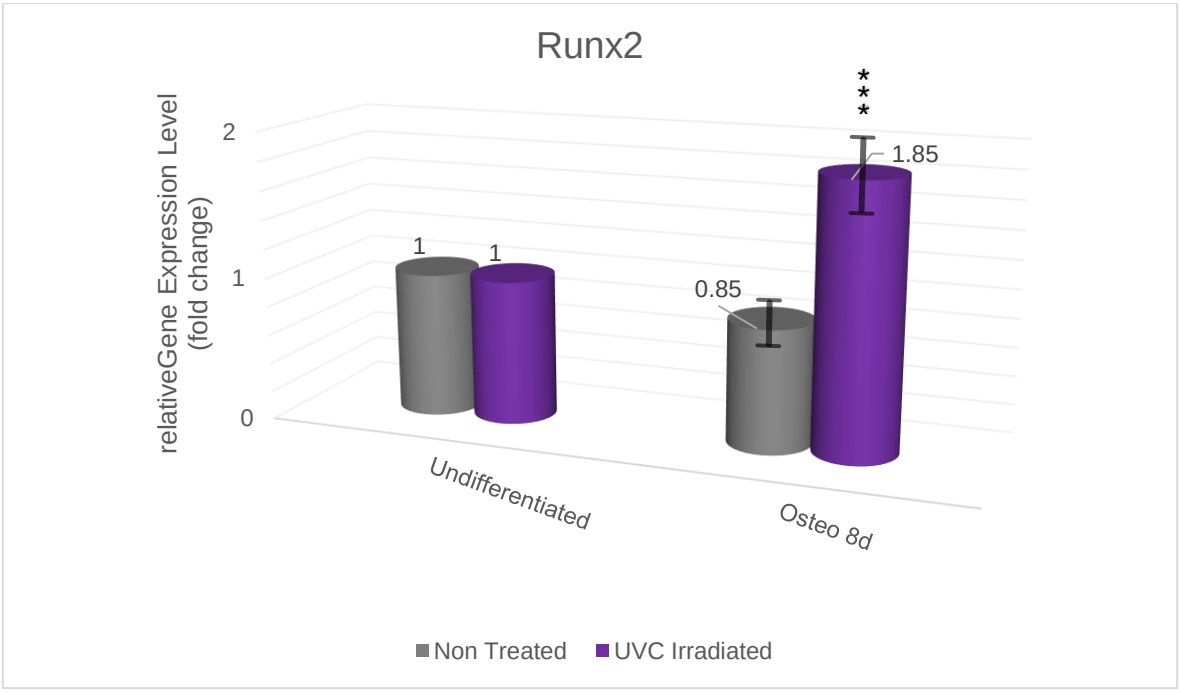

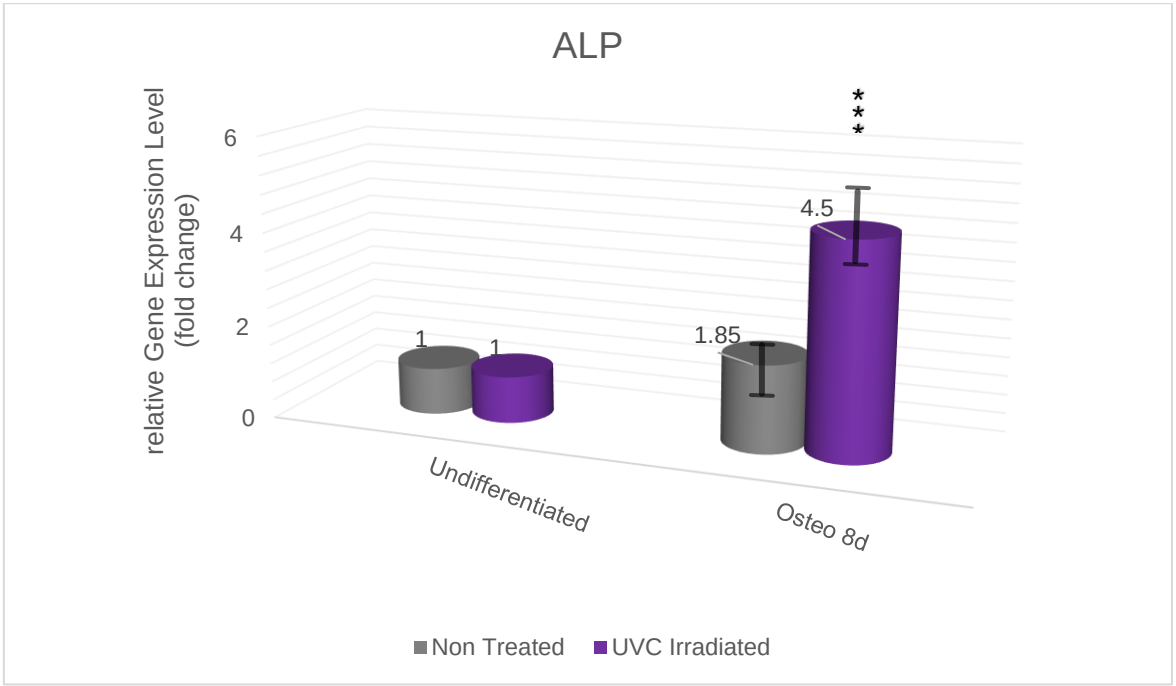

Figure 23 RT-PCR of the transcription factors RUNX 2 and ALP of the undifferentiated mMSC and after 8 days of proliferation. Results are shown as the mean. For statistical analysis for the RT-PCR results obtanied for the photofunctionalized discs were compared to the non-treated, used as control. *P < 0.05; **P < 0.01; ***P < 0.001

4. DISCUSSION

In the last decades dental implant therapies have been extensively developed and employed, however partial osteointegration, due to ageing, smoking and metabolic diseases, still remains a major issue. Titanium Oxide is the gold standard biomaterial used for the production of dental implants and the surface bio-activity of TiO_2 has been modulated by modifying its composition, topography and roughness. In addition, dental implants undergo biological aging, namely a contamination of titanium surface with hydrocarbons which reduces the osteointegration process, UVC irradiation (photofunctionalization) has been proposed as a mean to decontaminate TiO_2. The aims of this thesis have been to study the chemo-physical characteristics of titanium surfaces, as well as the mechanism and effects of the photofunctionalization process, which were not well defined yet.

4.1 CHEMIO-PHYSICAL CHARACTERIZATION OF TITANIUM SURFACES

Manipulation of titanium surfaces has been reported to improve bone apposition, tissue adhesion, and cell migration. Different rates of cellular attachment have been observed, following changes of the surface chemistry of titanium[41, 42]. However, little is known about the biochemical responses of cells to other surface properties, such as oxide thickness, oxide crystal structure, surface topography, or to the dynamic surface changes which can occur after implantation. In other words, implant surface preparation can significantly affect the properties of the surface which, in turn, can affect its interaction with the surrounding cells. Moreover, it is known that the micro-morphologic nature of the surface also plays an important role, as rough surfaces produce a tight interlock between cells and surface which stimulates cell differentiation [88]. Consequently, a considerable number of clinical studies have attempted to improve the quantity and quality of the bone-implant interface, in order to increase the success rate of endosseous implants. Titanium oxide is a quite simple material to be manipulated. For example, it can be treated by additive methods, such as the titanium plasma spray procedure, to increase surface area. Alternatively it can be modified by subtractive methods, such as acid pickling, acid etching, sandblasting and other small particle-blasting, in order to change the texture or to increase the effective surface area. Additive treatments are performed to create a convex morphology while subtractive mechanical treatments create a concave surface texture.

The development and use of these surface modifications have been based on the theory that improved osseointegration can be achieved by increasing the topography or roughness of the implant surface. In literature there are several in vitro and in vivo studies that have analyzed the short-term effects of surface modification on cell adhesion and morphology. An in vitro study by Wennerberg et al. compared a smooth-polished surface to a sand-blasted surface showing that the rough surface created pits that extended the implant surface area, were better covered by bone, as compared to smooth-polished surfaces. Moreover, it was reported that a higher percentage of osteoblast-like cells attach to sandblasted surfaces, as compared to the same surfaces polished with a 1 μm diamond paste [42]. These results have been confirmed by Passeri et al., who showed that rough sandblasted/acid etched surface with irregular morphology significantly favor the attachment of osteoblast-like cells, when compared to smooth and regular surfaces [89]. In subsequent studies, the effects of different surface treatments on osteoingration were analyzed in vivo, using various animal models. Buser et al. evaluated the influence of additive and subtractive treatment methods on the osteointegration of different implants placed in the metaphysis of tibia and femur of miniature pigs. After 3 and 6 weeks morphometric analysis was performed and significant differences in bone-implant interface was observed, among the differentially treated implants, that the highest BIC was found for the sandblasted/acid-etched surfaces (HCl/H_2SO_4) and hydroxyapatite-coated implants, and they concluded that increase of implant surface roughness is positively correlated with increased levels of bone-implant interface [88]. Another method to evaluate integration of an implant is the torque removal test. It is used to measure the critical torque threshold at which BIC is destroyed, thus providing indirect information regarding the BIC and the overall anchorage (osteointegration) of different implants. Cordioli et al. after placing titanium implants in the tibial metaphysis of rabbits with 4 different surface topographies found that the highest torque removal was found for the implant with the acid treated surface, in other words the implant with the roughest surface[90]. Similar results have been reported by Klokkevold et al. They analyzed the torque resistance to removal of titanium implants having an acid etched (HCl/H_2SO_4) surface (rough), as compared to machined surface implants, which are relatively smooth. Resistance to torque removal was found to be four times greater in etched implant. It was suggested that chemical etching of the titanium implant surface significantly increased the strength of osseointegration[91]. It is not clear yet whether additive methods of surface modification are better than subtractive ones. However, in the study of Cochran et al. it was found that a sandblasted and acid-etched titanium implant had a greater bone-to-implant contact than did a comparably-shaped implant with a titanium plasma sprayed surface[92].

Taken together, these studies provide evidence that surface modifications may result in a better osseointegration process. Nevertheless, even if these new surface treatments were shown to improve adhesion at the interface between implant and bone, the BIC still remains lower than 60% and no matter what surface modification is carried out, the surface seems to create a barrier for the cells [93, 94]. Therefore, microscopic changes of the surface are not sufficient to fully optimize the osseointegration process. However, the elegant study by Morra et al. provided evidence that the surface chemical composition also plays a critical role. Different commercially available implants were studied using the XPS technique and such analysis highlighted the presence of high levels of carbon onto their surfaces, reaching levels of even 75% of the outer surface [70, 95]. Ogawa et al. defined the appearance of carbon onto titanium as biological ageing and reported that it is an inevitable process occurring after titanium production [68].

In our study, we have thoroughly monitored the chemical composition of titanium oxide surfaces that had been pre-treated with different methods at the time of manufacture, this was undertaken before and after UVC irradiation, using complementary chemo-physical techniques.

Our analysis, performed on both dental implants and titanium discs showed a high level of carbon contamination (on average about 40% of the outer surface) in some cases reaching even 63%. Although high levels of carbon contamination had already been reported, our data provide more solid evidence, as in our experimental approach we analyzed the surface chemical composition at more than one depth. While by means of XPS, also employed in previous studies, the resolution was only of a few to 100 µm, with AES the resolution was situated in the 10 to 100 nm range, Moreover, we utilized also EDS because, even if it has a resolution similar to AES, it allows to analyze a bigger surface area. All the techniques confirmed the same chemical composition, with 40% of carbon, 35% of oxygen, 7% of Titanium and the rest being either part of the alloy or components used during surface modification treatment. In addition, to better understand the phenomenon of the presence of hydrocarbon on titanium surfaces, we performed the mapping of these elements, which had not been reported in literature. Such analysis has highlighted that carbon shows a non-homogeneous grain type distribution and that it is spread all over the analysed area, reaching an atomic concentration of even 63 % in some parts.

Ogawa et al. introduced a new method to remove carbon contamination, namely photofunctionalization. By exploiting UVC irradiation on titanium surfaces their studies reported a drastic decrease of carbon immediately after photofunctionalization [73, 77]. Our view is that biological ageing is not selective and that photofunctionalization decontaminates the surfaces independently of the geometry of the implant. In order to test our hypothesis, in this study we used commercially available titanium dental implants as well as titanium disks with different types of surface treatments, along with a different macroscopic geometry. On all the samples the amount of carbon deposition on the surface was almost identical as assessed by XPS and AES analysis **Table 6.** The peak recorded at 285 eV in the XPS spectrum corresponds to the presence of different C containing molecules on the surfaces. After UVC photofunctionalization this amount was greatly decreased, therefore in line with current literature. Moreover, the intensity of O and Ti peaks increased suggesting that an easier ionization of O and Ti atoms occurred on a less contaminated surface. By XPS analysis we observed that photofunctionalization was also able to decrease the fluoride contamination revealed by the CF_2 component of the C1s spectrum, probably originating from the acid-etching procedure during manufacturing.

It has been reported that biological ageing occurs within 4 weeks after implant production, and that after this time the contamination reaches a plateau [68]. In our study, titanium discs after UVC irradiation were left at atmospheric conditions for a period of 10 weeks and monitored through XPS analysis, particularly focusing on the levels of carbon, oxygen and titanium. Immediately after UVC irradiation the carbon / titanium ratio decreased of about 3 folds. Exposure of the surface to the atmosphere led to a logarithmic increase in the amount of carbon within 10 weeks. Interestingly, after 6 weeks the carbon contamination reached the initial level, and it actually continued to increase to a higher level before reaching a final plateau. Therefore, our results appear somehow different from the data previously reported by Ogawa et al. [68, 77]. Such difference may be accounted for by different UVC irradiation protocols used in the two studies. We developed a faster and therefore handier photofunctionalization procedure, which can be more easily applied chairside. In our study the surfaces were irradiated for only 12 minutes while in the other studies the surfaces were irradiated for 24 hrs.

An additional observation drawn from our analysis is that UVC irradiation created a rapid decrease of the O/Ti ratio and a biphasic behavior of the Oxygen level in relation to time. In the first time range, going from time 0 (immediately after UVC irradiation) to 4 weeks the level of oxygen on the TiO_2 discs increased Figure 11. In contrast, in the second range, between

4 and 10 weeks of surface exposition to the atmosphere, the level of the oxygen ratio remains quite stable.

Photofunctionalization does not completely remove the presence of hydrocarbon chains, due to biological aging, however it affects the physical properties of the surfaces resulting in an increased wettability, which provides a predictive index of cytocompatibility and cell adhesion.

Measurement of the wettability of a material is expressed by the contact angle between a fluid, typically distilled water, and its surface. Decreasing the contact angle (i.e. increasing wettability) has been reported to enhance the interaction between the implant surface and the surrounding biological micro-environment [33, 96]. During the early stage of cell attachment, microvilla and filipodia play a critical role, their presence is modulated and their migration indicates high cell activity [97]. In our study cells cultured on UV treated surfaces were increased in number, supporting the positive effect of decontaminating titanium surfaces. Cell attachment to a biomaterial is closely related to its surface energy, for this reason the development of new implant surfaces has been mainly focused on the control of the wettability of the implant fixture. In previous studies, as detailed below, the wettability of materials and their effects on the cells was described, but failed to clearly define the phenomenon and did not explain the effect caused by surface configuration of the crystalline structure of surface oxides.[47, 98].

Thus, the results obtained in this thesis have significantly contributed to elucidate the phenomenon, discussing it from a chemo-physical point of view. Yanagisawa et al. [99] reported that the contact angles (θ) of materials affected both the cell attachment and spreading rates ($d\theta/dt$). With small contact angles and high wettability, the cell attachment rate was high, while it was low when the contact angles were large and wettability was low. Thus, they concluded that wettability of biomaterials is considered an important parameter of biological effect at the cell level. Only a few investigations have related the influence of surface roughness and crystalline structure on wettability and cells spreadability [96]. It was suggested that the wettability and spreadability are related to the crystalline structure of the oxide film formed on these biomaterials. In those studies, shot peening, a technique similar to sandblasting, was utilized to create a controlled surface oxide topography, which, without changing the crystal

structure of the surface, was able to change the oxide layer. It was speculated that the surface energy (monitored by the contact angle measurement) relates to the crystalline structure of surface oxide films. It was also observed, for shot peening and pre-oxidized surfaces, that changes in contact angles as a function of time are strongly dependent upon the type of surface oxide. A higher spreading rate is observed on biomaterials whose surfaces are covered with TiO_2, while a lower spreading coefficient is seen on cubic structure oxides including spinel type oxide formed on stainless steel [100].

Also Ogawa et al. reported an increase in wettability after UVC irradiation of titanium implants, however the mechanisms governing such an important change have not been fully elucidated [77]. During our XPS analysis we detected a peak at 534 eV corresponding to H_2O molecules [95, 101], which attach onto the surface when exposed to the atmosphere, after production or when removed from the UVC device and placed in the analysis apparatus producing an oxidation of Ti^{3+} to Ti^{4+} [102]. However, we observed that after UVC irradiation there was a decrease in the amount of H_2O and an increase in the amount of TiOH. The reason is that UVC photon energy induced a one-electron oxidation with water to produce a hydroxyl radical OH and dissociation of H^+ [103]. Wettability is dependent on the hydrogen bonding network formed on the surface after hydrocarbon decontamination, because the hydroxyl groups together with the O Vacancies, present on an almost all carbon free surface are able to form more OH^- groups. In other words, the bridging oxygens on the outer surface after carbon decontamination are forming weak hydrogen bonds with the hydrogen present in the molecules of H_2O in blood. At the same time, the Ti atoms present on the surface, which for their incomplete electron coordination are slightly positive, can favorably interact with the oxygen atoms which are slightly negative and present in the water molecules. Our results show that after UVC treatment, (photofunctionalization), the surface is clean and there is a thin outer layer of water, which increases both the wettability of the surface and favors protein attachment.

Fig. 24 , illustrates a theoretical model that we developed to summarize the effects of the chemo-adsorption process of hydrocarbons on TiO_2 ("biological ageing"), and the role of photofunctionalization in as far as cleaning and enhancing the TiO_2 surface. When exposed to atmosphere, TiO_2 surfaces can bind pollutant hydrocarbons through interactions with carboxyl

and amine groups. The surface shown in the Figure is TiO_2 (110), and it is an example of the different faces present in the polycrystalline oxide on the implant surface. Carboxyl and amine groups are taken into consideration since they are typical groups exhibited by amino acid side chains in protein structure. The left panel shows the interaction between C=O groups typical of gaseous contaminants present in the atmosphere (e.g. volatile aldehydes) with the penta-coordinated Ti exposed on the implant surface. The dotted line indicates that the interaction (chemo-adsorption) is one order of magnitude weaker than the typical bond energy in organic molecules. The prolonged exposure to UV photons – much higher in energy as compared to visible light – is able to break such weak "bonds", thus removing the contaminants from the surface and re-establishing a clean surface (central panel). The schematic representation also shows the partial charges present on the surface (+/– delta), due to the difference in electronegativity of Ti as compared to O atoms. The deprotonated carboxyl groups (COO^-) and protonated amine groups (NH_3^+) typically present in aqueous environment can easily interact with such partial charges present on the photofunctionalized surface, thus enhancing the anchorage of proteins (right panel). The bi-dentate interaction between COO^- and two contiguous Ti atoms has been proven very effective from this point of view [21-31][95].

In clinical practice the possibility of achieving a direct bond between titanium and amino acids can have a great impact in terms of tight adhesion of the cells to the surface. As a result, osteointegration would be enhanced providing for a more stable implant, that would improve the long term survival rate of the implants. Especially beneficial could be its use in cases of poor bone quality due to age or disease. In addition, it can be expected that the exposure of all implants to the same type of photofunctionalization procedure before use will create the same standard starting conditions in all patients, thus allowing the clinician to make more accurate comparisons of the individual outcomes.

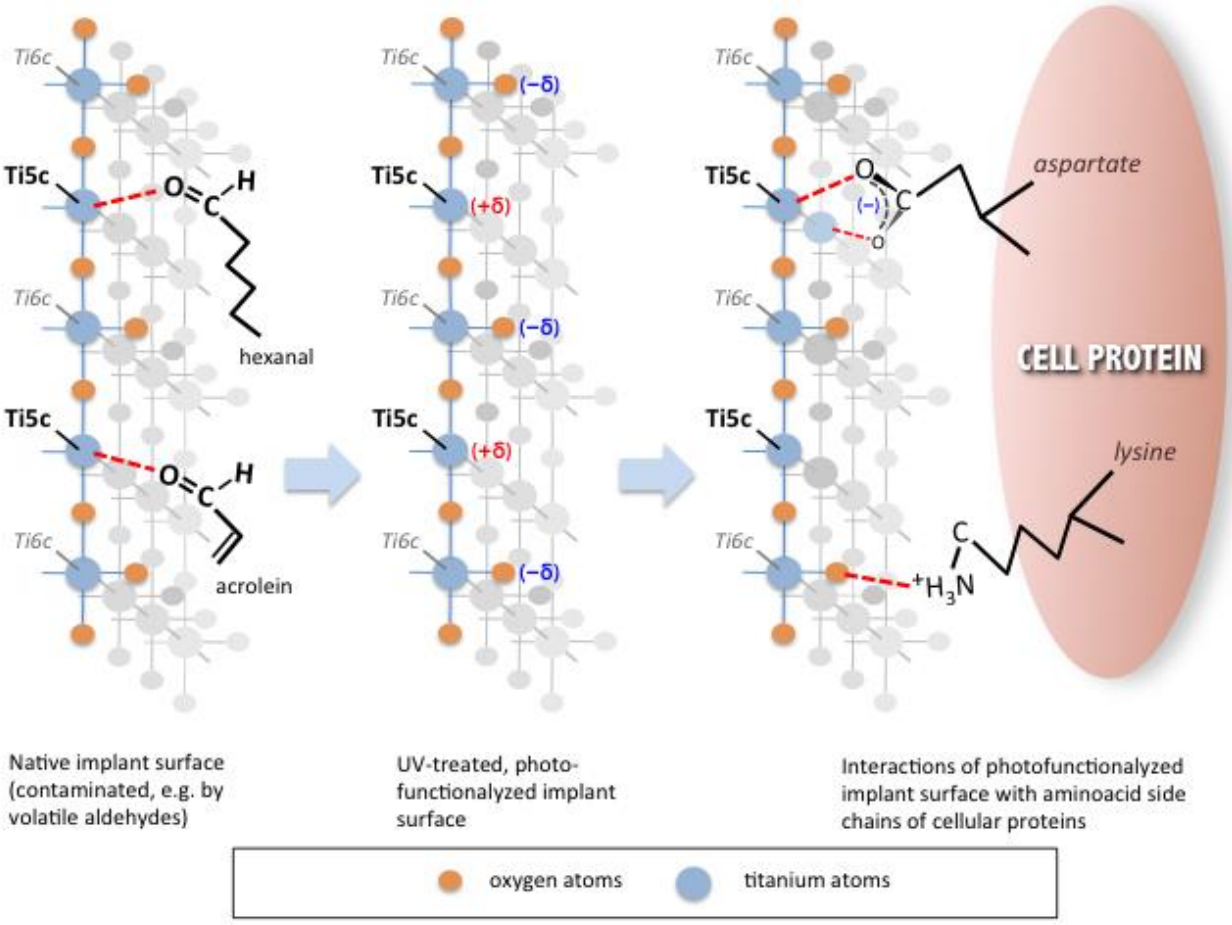

Figure 24 Scheme representing the interactions of carboxyl and amine groups with the TiO_2 surface when exposed to the atmosphere. The surface shown is TiO_2 (110), with Ti (light blue) and O (orange). See text for details

A number of reports, focused on the biological effects of various surface modifications, have highlighted an inverse correlation between proliferation and differentiation rates of osteoblasts [104, 105]. There is evidence showing that micro-roughened titanium surfaces have advantages over machined smooth surfaces in increasing both tissue-titanium mechanical interlocking and osteoblastic differentiation [106], thus resulting in faster bone formation [107]. However, other studies have shown that the bone mass formed around rough surfaces is smaller than the one formed around machined ones [106], indicating that rougher surfaces of material substrates reduce cell proliferation[98, 108-110]. Therefore, it appeared that a surface modification sustaining both osteoblast proliferation and differentiation was not available yet, and that only a compromise could be achieved. Here comes into play the importance of photofunctionalization, as results have demonstrated that UVC irradiation of both rough and smooth surfaces enhance the rate of both osteoblast proliferation and differentiation.

In most studies cell attachment/proliferation on photofunctionalized surfaces was assessed at 3-24 hours, using cell lines on Gr 2 TiO_2. In all reports a greater number a greater number of cells (on average a two fold increase) has been reported to adhere/grow onto UVC irradiated surfaces, as compared to untreated surfaces. In our experiments, we have used a different strategy to assess the effect of photofunctionalization on cell adhesion/proliferation and differentiation. First, we have used not only the pre-osteoblastic cell line MC3T3, but also primary stem/precursor cells derived from murine bone marrow. In addition we have compared titanium surfaces pre-treated in different ways, before and after UVC treatment. Second, we have compared TiO_2 disks of a different grade of purity. In our study we have analysed titanium grade 2, because it was previously utilized by the other groups, and titanium grade 4, as in the clinical practice only titanium grade 4 is used because of its mechanical properties. Furthermore, to make the study more reliable and standardized, the surfaces were not treated in the lab as, in the previous reports, but directly by the implantology company to simulate the clinical practice. Third, we have monitored cell survival/proliferation and differentiation not only at short times (24hours), but also up until 8 days of culture onto different surfaces. Our data, obtained seeding the pre-osteoblastic cell line onto Gr 2 machined or sand-blasted acid etched, and Gr 4 sand-blasted acid etched discs, have demonstrated in all cases the positive effect of photofunctionalization, resulting in an increased cell attachment/proliferation of about 2 to 3 folds, after 24 hours. Such effect is in line with previously reported data [62, 80].

Moreover, on the same discs, we evaluated also the percentage of dead cells and observed different outcomes in the different types of discs. Following UVC irradiation, there were virtually no dead cells on the Gr 2 machined discs, while on Gr2 sand-blasted acid etched discs a similar percentage of dead cells was detected as in non-irradiated discs, and on Gr 4 sand-blasted acid etched discs we observed a two third reduction. Overall, photofunctionalization of Gr 4 sand-blasted acid etched surfaces, which are currently employed in dental implants , showed an encouraging effect for its clinical application. This conclusion is supported also by fluorescence microscope analysis imaging Fig. 20 which shows a higher number of cells on the irradiated surface, as compared to the non irradiated one.

Furthermore, in our study, the novel use of primary MSCs, which better mimic the situation in vivo, has confirmed the beneficial effect of photofunctionalization on cell adhesion/growth after 24 hrs of culture, and provided evidence that such effect is even stronger in a longer term Fig. 21 During 8 days of culture the ratio between viable cells present on irradiated vs non irradiated surfaces was progressively higher, and, remarkably, at the end point of our analysis (8 days) a minority of cells (4%) were present on non photofunctionalized discs, as compared to the percentage (96%) detected on UVC treated discs. These results represent a significant extension and improvement of a previous observation by Aita who was the only group that compared the growth of human MSCs onto irradiated and non irradiated surfaces. They reported that after 7 days of culture the amount of cells present on UV irradiated discs was increased by 3-4 folds [75].

We also compared the osteogenic ability of mMSCs cultured on UVC irradiated or non irradiated Gr 4 sand-blasted acid etched discs. Osteogenic differentiation was assessed by monitoring gene expression of two key osteogenic markers, Runx2 and ALP, using quantitative Real-Time PCR. Runx2 is a master gene of osteogenesis, as it plays a pivotal role in the commitment of multipotent mesenchymal cells to the osteoblastic lineage, and is required at early stages of osteoblast differentiation. Moreover, it is able to up-regulate the expression of many bone matrix protein genes, including type 1 collagen, osteopontin, bone sialoprotein and osteocalcin. Thus, analysis of *Runx2* expression is crucial to determine the onset of the molecular cascade of events that orchestrate osteogenic differentiation. Previous studies have shown that days 3 and 8 after osteogenic induction are optimal time points at which to prove that the osteogenic process is taking place [87]. Therefore, we compared the expression of both Runx2 and ALP in MSCs seeded onto UVC irradiated or non irradiated discs, at day 3

and 8 after osteogenic induction. ALP has been one of the first key players in the process of osteogenesis to be recognized. For this reason it is a marker currently used to evaluate osteogenic differentiation when assessing the phenotype or developmental maturity of mineralized tissue cells. In literature it has been reported a constant increased of its expression after UVC irradiation of the surface after 3, 7 and 10 days. Our results have confirmed the up-regulation of ALP expression at both day 3 (cells grown on all surfaces, including plastic dishes, used as internal controls) and day 8, particularly in MSCs seeded onto photofunctionalized discs. Interestingly, Runx2 expression has not been previously reported in literature, and our data provide the first evidence that its transcriptional activity is greatly enhanced in cells induced to differentiate onto UVC irradiated surfaces. An increased expression by 2 folds at both time points is rather relevant, as it is known that changes in gene expression of transcription factors are rather limited, as compared to variations occurring in the transcription of enzymes (such as ALP). Our results also suggest Runx2 is a more reliable marker than ALP, which is known to be variable, mainly at early times of osteogenesis.

The improved survival/proliferation and differentiation of cells cultured onto photofunctionalized discs may be accounted for by observations reported by Iwasa et al.[111]. In his study, confocal microscopic images of osteoblasts after staining with rhodamine phalloidin showed that after 3 hours of incubation the cells seeded onto UV-treated titanium surfaces appeared definitely flatter and larger than the ones seeded on untreated surfaces. Moreover, cells on UV treated titanium surfaces showed a clear stretch of lamellipodia-like actin projections and cytoskeleton within their cytoplasm, whereas the majority of cells on the untreated surfaces were round and did not exhibit the initiation of elongating cell processes and developing cytoskeleton [111].

From a chemo-physical point of view it could be speculated that the carboxylic group present on the terminal of the protein structures gets attracted by the surface, thus resulting in a larger surface covered by cells, increasing the BIC and in turn creating a stronger osteointegration.

These results suggest that the surfaces used in dental implantology can still be improved and that titanium after UVC-irradiation enables an increase in osteoblastic proliferation without sacrificing differentiation. This biological advantage was well shown by the higher cell number

of mMSC detected after 8 days of culture on photofunctionalized disks, along with their increased expression of osteogenic markers. It can be speculated that such improved cell functions may be due to an improved interaction between titanium surface and cell adhesion proteins Fig. 23. In literature there is evidence supporting this view. Elias et al. analyzed the relationship between implant surface wettability and cytokine production by blood cells [96]. In particular, on hydrophobic surfaces it was detected the presence of antibodies that could reduce cell adhesion. In contrast, both thrombins and prothrombins were predominant on the hydrophilic surfaces, and it is well known that these proteins play an important role in stimulating cell adhesion to the biomaterial surface. In particular, it has been shown that thrombin may become conformationally altered in the post clotting wound environment, thus exposing the amino acid sequence (RGD) capable of interacting with the cell surface integrins, which would result in increased ability of the cells to adhere to the photofunctionalized surface [112]. In turn, it has been reported that the integrin attachment has a direct role in modulating the expression of genes involved in both cell proliferation and differentiation gene expression [113, 114]. Therefore, there is scientific evidence that after carbon removal the number of binding sites for surface proteins is increased and in turn improves the expression of genes that control cell proliferation and differentiation. Taken together, these findings can change the approach to study implant surfaces and their modifications, by focusing on the biophysical interactions between cell proteins and titanium surfaces. Our studies have contributed to gain insights into the mechanisms that underlie biological ageing and the effects of UVC irradiation. Photofunctionalization is certainly a new strategy in producing a more reactive and biocompatible surface independently from the surface treatments performed during manufacturing.

5. CONCLUSION

- The XPS and AES study demonstrated that, the hydrocarbon deposition, known as biological ageing of TiO_2, is inevitable no matter which the surface treatment carried out during manufacturing. This could be a major reason of incomplete osteointegration leading to a low level of BIC or even to unsuccessful osteointegration.

- Furthermore, the chemo-physical analysis has shown that Photofunctionalization is a valid method to reverse biological ageing. The results indicate that 12 minutes of UVC irradiation provides an easy and efficient means to remove the hydrocarbons contamination from titanium dental implants without altering the topography of the surface.

- Titanium surfaces after UVC irradiation have given data that show an increase in the cell attachment/proliferation and decrease the amount of dead cells indicating that an almost carbon free surface is more biocompatible. Moreover, the increase in cell count found a positive correlation with the osteointegration master gene RUNX2.

- The results raised that hypothesis that UV-induced changes in chemical structure of the surface can explain the positive biological effects. The energy carried by UV rays is able to break the bonds between Ti5c atoms and the O and/or N atoms of contaminant molecules. Chemically active Ti5c sites then become available for the attachment to O, N, S atoms present in any protein, leading to improved biocompatibility of the implant and integration. The data suggest a new model of interaction between implant surface and adsorbed molecule based not only on the surface charge but also on their atomic geometry.

- The study may provide a valid base for a clinical trial of photofunctionalization. As we must consider that life expectancy is increasing and along with it systemic diseases which impair cell metabolism. Being able to increase the level of osteointegration with photofunctionalization would improve the quality of life of many patients, who are

presently rehabilitated with removable partial or complete dentures, because a fixed solution with implants is considered contraindicated.

ABSTRACT

Dental implantology has become the gold standard in the rehabilitation of the patients with partial or full edentulous conditions. However, there still are some contraindications regarding the placement of dental implants in patients with systemic diseases, like diabetes, osteoporosis etc. which impair bone metabolism. That is, even if the success rate of the integration of dental implants is rather high it still remains far from ideal. Looking at a more microscopical level the fixture of an implant after a successful process of healing, known as osteointegration, is in contact with the bone only for a 40-60 % of its surface. This seems to be far from ideal, thus in the past years many different researchers have tried to manipulate and modify the TiO_2 surface to improve the BIC even though without success in reaching higher BIC levels. This study analyzes different TiO_2 surfaces to demonstrate the inevitable presence of hydrocarbon on the surfaces. Thanks to the physical analysis performed, namely XPS and AES it has been possible to demonstrate that besides the atoms of Ti and O the surface is covered by a layer of hydrocarbons resulting in its contamination. This discovery could help answer the question as to why the BIC is far from an ideal 100%. That is, a low level of stem cells cannot interact with the surface of the fixture because of the presence of hydrocarbon chains on it which are making it hydrophobic in character and block the cell membrane proteins from attaching to the surface. It was therefore necessary to find a way to decontaminate the surface. In this study 12 minutes UVC- irradiation of the TiO_2 surface, known also as photofunctionalization, has been utilized. After this process the chemo-physical analysis, XPS AES AFM, were performed and the results were compared to the ones obtained before the UVC irradiation. There was a clear decrease in hydrocarbon contamination and the hydrophobic surface became super-hydrophilic. These positive results led to the necessity of performing the in vitro biological studies, to confirm a better biocompatibility of the TiO_2 after UVC-irradiation with the osteoblasts. As for the physio-chemical studies and also in the biological studies more types of surfaces of TiO_2 were utilized. Also were used both a cell line MC3T3 and a primary cells m-MSC (murine, mesenchymal stem cells). This decision was made because the aim of the study is to demonstrate the presence of hydrocarbons on every TiO_2 surface independently of the surface manipulation during manufacturing. In the first part of the study MC3T3 were cultured for 24 hrs. onto

titanium discs before and after UVC irradiation, then cell count was performed. After UVC-irradiation an increase of living cells was noticed and even more interesting a decrease in dead cells in the culture media was reported. The study proved that more cells can reach the TiO_2 surface after UVC- irradiation and that the attachment capability of the cells is enhanced. The study was repeated for the m MSC but with different time points; undifferentiated, 12 hours, 24 hours and 8 days after differentiation. At every time point the amount of living cells on the UVC irradiated surface was higher. Moreover, at 3 and 8 days after differentiation a gene expression analysis was performed, by analyzing the expression of ALP as a marker of bone activity and the master gene of bone formation RUNX2. The results found correlation with the cell count demonstrating that UVC irradiation improves the osteoblasts attachment and their activity during the first phase of osteointegration. All these studies led to the formulation of a model to explain this phenomena. Specifically, TiO_2 after UVC-irradiation becomes decontaminated of its hydrocarbons and becomes highly reactive due to a missing bond to fully coordinate its molecule. If left at atmospheric conditions it would inevitably react quite fast as the carboxylic group (COO-) present on the terminal chain of the hydrocarbons; which fits by charge and geometry perfectly on the outer layer of molecule. However, if placed in contact with blood the highly reactive TiO_2 surface is free to interact with the carboxylic group present on the terminal portion of the amino acids which compose the proteins (integrins) present on outer membrane of cells. After UVC-irradiation the sites to which the proteins can interact with the surface of the dental implants is greatly enhanced. Increasing the contact of the cell integrins with the implant surface is responsible for the increase in gene expressions inside the cell which in turn will improve and speed up the process of osteointegration.

STRESZCZENIE

Implantologia stomatologiczna jest dziś złotym standardem w rehabilitacji pacjentów z chorobami powodującymi częściową lub całkowitą utratę uzębienia. Nadal istnieją jednak pewne przeciwwskazania do wszczepiania implantów stomatologicznych u pacjentów z chorobami układowymi, jak np. cukrzyca czy osteoporoza, które powodują zaburzenia metabolizmu. W takich przypadkach skuteczność integracji implantów stomatologicznych nigdy nie jest idealna, a co najwyżej stosunkowo wysoka. Na poziomie bardziej mikroskopijnym, element mocujący implantu ma po skutecznym procesie gojenia, nazywanym osteointegracją, kontakt z kością jedynie na 40–60% powierzchni. Jest to stan daleki od ideału, dlatego w ostatnich latach wielu badaczy próbowało przetwarzać i modyfikować powierzchnię TiO_2 tak, aby zwiększyć powierzchnię kontaktu kości a implantem (BIC – *Bone to Implant Contact*), nie osiągnęli jednak wyższych wartości BIC. Niniejsze badanie analizuje różne powierzchnie TiO_2, by wykazać nieuniknioną obecność węglowodów na takich powierzchniach. Przeprowadziwszy analizy fizyczne, czyli XPS i AES, mogliśmy wykazać, że powierzchnia pokryta jest nie tylko atomami Ti i O, ale również warstwą węglowodorów powodującą skażenie powierzchni. Odkrycie to może ułatwić uzyskanie odpowiedzi na pytanie, dlaczego wartość BIC jest daleka od idealnych 100%. Mianowicie niski poziom komórek macierzystych nie może reagować z powierzchnią mocowania, ponieważ obecne na implancie łańcuchy węglowodorowe nadają mu charakter hydrofobowy i blokują przyłączanie białek błony komórkowej do powierzchni. Dlatego konieczne było znalezienie sposobu odkażenia powierzchni. W tym badaniu zastosowano 12-minutowe napromieniowani powierzchni TiO_2 promieniami UVC, nazywane fotofunkcjonalizacją. Po tym procesie przeprowadzono analizę fizykochemiczną, XPS AES AFM, a wyniki porównano z wynikami uzyskanymi przed napromieniowaniem UVC. Zaobserwowano wyraźną redukcję skażenia węglowodorami, a powierzchnia hydrofobowa stała się super-hydrofilowa. Po uzyskaniu owych pozytywnych wyników konieczne stało się przeprowadzenie badań biologicznych *in vitro* mających na celu zwiększenie biokompatybilności TiO_2 z osteoblastami po napromieniowaniu UVC. W badaniach fizykochemicznych oraz biologicznych zastosowano więcej rodzajów powierzchni TiO_2. Użyto też zarówno linii komórkowej MC3T3 jak i m-MSC (mysich mezenchymalnych komórek

macierzystych). Taką decyzję podjęto, ponieważ celem niniejszego badania jest wykazanie obecności węglowodorów na każdej powierzchni TiO_2 niezależnie od przetworzenia powierzchni w trakcie produkcji. W pierwszej części badania komórki MC3T3 hodowano przez 24 godziny na płytkach tytanowych przed i po napromieniowaniu UVC, następnie sprawdzono liczbę komórek. Po napromieniowaniu UVC zauważono zwiększenie liczby komórek żywych, a co jeszcze bardziej interesujące, odnotowano zmniejszenie liczby martwych komórek w pożywkach. Badanie dowiodło, że po napromieniowaniu UVC większa liczba komórek może dotrzeć do powierzchni TiO_2, a zdolność komórek do przyłączenia jest zwiększona. Badanie powtórzono z zastosowaniem mMSC, ale z innymi punktami czasowymi: przed różnicowaniem, 12 godzin, 24 godziny i 8 dni po różnicowaniu. W każdym punkcie czasowym ilość żywych komórek na powierzchni poddanej promieniowaniu UVC była większa. Ponadto po 3 i 8 dniach od różnicowania przeprowadzono analizę ekspresji genów poprzez analizę ekspresji ALP jako markera aktywności kości i genu nadrzędnego tworzenia się kości (RUNX2). Wyniki ujawniły powiązanie z liczbą komórek wykazujące, że promieniowanie UVC zwiększa łączenie osteoblastów i ich aktywność w pierwszej fazie osteointetgracji. Wszystkie te badania doprowadziły do sformułowania modelu wyjaśniającego owe zjawisko. Po napromieniowaniu UVC TiO_2 zostaje odkażony z węglowodorów i z powodu brakującego wiązania staje się wysoko reaktywny, dążąc do pełnego skoordynowania cząsteczki. Pozostawiony w warunkach atmosferycznych nieuchronnie dość szybko reagowałby z grupą karboksylową (COO-) obecną w końcowym łańcuchu węglowodorów, której ładunek i geometria idealnie pasują do warstwy zewnętrznej cząsteczki. Natomiast w kontakcie z krwią wysokoreaktywna powierzchnia TiO_2 może reagować z grupą karboksylową obecną w końcowej części aminokwasów tworzących białka (integryny) obecne na zewnętrznej błonie komórek. Po napromieniowaniu UVC obszar, na którym białka mogą reagować z powierzchnią implantów stomatologicznych, jest znacznie zwiększony. W rezultacie kontakt integryn komórek z powierzchnią implantu się zwiększa, a to powoduje zwiększenie ekspresji genów wewnątrz komórki, co z kolei poprawia i przyspiesza proces osteointegracji.

BIBLIOGRAPHY

1. Roy, M. and w. Hędzelek, *Photofunctionalization: a new method to bio-activate the titanium implant surface – review of literature.* Journal of Stomatology (Czasopismo Stomatologiczne), 2014. **67**(5): p. 682-691.
2. Lee, C.T., et al., *Survival analysis of wide dental implant: systematic review and meta-analysis.* Clin Oral Implants Res, 2016. **27**(10): p. 1251-1264.
3. Norowski, P.A., Jr. and J.D. Bumgardner, *Biomaterial and antibiotic strategies for peri-implantitis: a review.* J Biomed Mater Res B Appl Biomater, 2009. **88**(2): p. 530-43.
4. Porter, J.A. and J.A. von Fraunhofer, *Success or failure of dental implants? A literature review with treatment considerations.* Gen Dent, 2005. **53**(6): p. 423-32; quiz 433, 446.
5. Annunziata, M. and L. Guida, *The Effect of Titanium Surface Modifications on Dental Implant Osseointegration.* Front Oral Biol, 2015. **17**: p. 62-77.
6. Branemark, P.I., et al., *Intra-osseous anchorage of dental prostheses. I. Experimental studies.* Scand J Plast Reconstr Surg, 1969. **3**(2): p. 81-100.
7. Albrektsson, T., et al., *Osseointegrated titanium implants. Requirements for ensuring a long-lasting, direct bone-to-implant anchorage in man.* Acta Orthop Scand, 1981. **52**(2): p. 155-70.
8. Schroeder, A., *[Biology of the implant as foreign body].* Schweiz Monatsschr Zahnmed (1984), 1985. **95 Spec No**: p. 841-6.
9. Fini, M., et al., *Osteoporosis and biomaterial osteointegration.* Biomed Pharmacother, 2004. **58**(9): p. 487-93.
10. Ku, Y., C.P. Chung, and J.H. Jang, *The effect of the surface modification of titanium using a recombinant fragment of fibronectin and vitronectin on cell behavior.* Biomaterials, 2005. **26**(25): p. 5153-7.
11. Schenk, R.K. and D. Buser, *Osseointegration: a reality.* Periodontol 2000, 1998. **17**: p. 22-35.
12. Meyer, U., et al., *Ultrastructural characterization of the implant/bone interface of immediately loaded dental implants.* Biomaterials, 2004. **25**(10): p. 1959-67.
13. Murai, K., et al., *Light and electron microscopic studies of bone-titanium interface in the tibiae of young and mature rats.* J Biomed Mater Res, 1996. **30**(4): p. 523-33.
14. Franchi, M., et al., *Biological fixation of endosseous implants.* Micron, 2005. **36**(7-8): p. 665-71.
15. Probst, A. and H.U. Spiegel, *Cellular mechanisms of bone repair.* J Invest Surg, 1997. **10**(3): p. 77-86.
16. Mavrogenis, A.F., et al., *Biology of implant osseointegration.* J Musculoskelet Neuronal Interact, 2009. **9**(2): p. 61-71.
17. Chappard, D., et al., *The early remodeling phases around titanium implants: a histomorphometric assessment of bone quality in a 3- and 6-month study in sheep.* Int J Oral Maxillofac Implants, 1999. **14**(2): p. 189-96.
18. Davies, J.E., *Mechanisms of endosseous integration.* Int J Prosthodont, 1998. **11**(5): p. 391-401.
19. Goutam M, C.G., Mishra SK, Singh M, Tomar BS, *Factors affecting Osseointegration: A Literature Review.* J Orofac Res, 2013. **3**(3): p. 5.
20. Williams, D.F., *The Williams Dictionary of Biomaterials*. 1999: Liverpool University Press.

21. Park, J.L., R. S., *An introduction*. Third edition ed. biomaterials. 2007, New York: Springer New York. 1-16.

22. Roy, M., M. Idzior-Haufa, and W. Hedzelek, *Precision Attachments: A Review to Guide Clinicians.* Dental and Medical Problems, 2016. **53**(4): p. 559-565.

23. Roy, M., et al., *Photofunctionalization of dental zirconia oxide: Surface modification to improve bio-integration preserving crystal stability.* Colloids Surf B Biointerfaces, 2017. **156**: p. 194-202.

24. Wenz, H.J., et al., *Osseointegration and clinical success of zirconia dental implants: a systematic review.* Int J Prosthodont, 2008. **21**(1): p. 27-36.

25. Andreiotelli, M., H.J. Wenz, and R.J. Kohal, *Are ceramic implants a viable alternative to titanium implants? A systematic literature review.* Clin Oral Implants Res, 2009. **20 Suppl 4**: p. 32-47.

26. Osman, R.B., et al., *Ceramic implants (Y-TZP): are they a viable alternative to titanium implants for the support of overdentures? A randomized clinical trial.* Clin Oral Implants Res, 2014. **25**(12): p. 1366-77.

27. Cordeiro, J.M. and V.A. Barao, *Is there scientific evidence favoring the substitution of commercially pure titanium with titanium alloys for the manufacture of dental implants?* Mater Sci Eng C Mater Biol Appl, 2017. **71**: p. 1201-1215.

28. Tengvall, P. and I. Lundstrom, *Physico-chemical considerations of titanium as a biomaterial.* Clin Mater, 1992. **9**(2): p. 115-34.

29. Breme, J., E. Eisenbarth, and V. Biehl, *Titanium and its Alloys for Medical Applications*, in *Titanium and Titanium Alloys*. 2005, Wiley-VCH Verlag GmbH & Co. KGaA. p. 423-451.

30. Lausmaa, J., *Surface oxides on titanium : preparation, characterization and biomaterial applications*. 1991, Department of Physics, Chalmers University of Technology, University of Göteborg: Göteborg.

31. Leyens, C., *Oxidation and Protection of Titanium Alloys and Titanium Aluminides*, in *Titanium and Titanium Alloys*. 2005, Wiley-VCH Verlag GmbH & Co. KGaA. p. 187-230.

32. Sutherland, D.S., et al., *Surface analysis of titanium implants.* Biomaterials, 1993. **14**(12): p. 893-9.

33. Feng, B., et al., *Characterization of surface oxide films on titanium and bioactivity.* J Mater Sci Mater Med, 2002. **13**(5): p. 457-64.

34. D., D.J., *Corroswion: Materials*. Vol. 2. 1990, Ohio: ASM International.

35. Kasemo B., L.J., *Surface science aspects on inorganic biomaterials. CRC Crit. Rev.Biocompat.* 1986. **2**: p. 45.

36. Albrektsson, T. and A. Wennerberg, *Oral implant surfaces: Part 1--review focusing on topographic and chemical properties of different surfaces and in vivo responses to them.* Int J Prosthodont, 2004. **17**(5): p. 536-43.

37. Schwartz, Z., et al., *Effect of titanium surface roughness on chondrocyte proliferation, matrix production, and differentiation depends on the state of cell maturation.* J Biomed Mater Res, 1996. **30**(2): p. 145-55.

38. Shalabi, M.M., et al., *Implant surface roughness and bone healing: a systematic review.* J Dent Res, 2006. **85**(6): p. 496-500.

39. Becker, W., et al., *A prospective multicenter clinical trial comparing one- and two-stage titanium screw-shaped fixtures with one-stage plasma-sprayed solid-screw fixtures.* Clin Implant Dent Relat Res, 2000. **2**(3): p. 159-65.

40. Junker, R., et al., *Effects of implant surface coatings and composition on bone integration: a systematic review.* Clin Oral Implants Res, 2009. **20 Suppl 4**: p. 185-206.

41. Wennerberg, A., T. Albrektsson, and B. Andersson, *Bone tissue response to commercially pure titanium implants blasted with fine and coarse particles of aluminum oxide.* Int J Oral Maxillofac Implants, 1996. **11**(1): p. 38-45.

42. Wennerberg, A., et al., *A histomorphometric and removal torque study of screw-shaped titanium implants with three different surface topographies.* Clin Oral Implants Res, 1995. **6**(1): p. 24-30.

43. Wennerberg, A., T. Albrektsson, and J. Lausmaa, *Torque and histomorphometric evaluation of c.p. titanium screws blasted with 25- and 75-microns-sized particles of Al2O3.* J Biomed Mater Res, 1996. **30**(2): p. 251-60.

44. Testori, T., et al., *A prospective multicenter clinical study of the Osseotite implant: four-year interim report.* Int J Oral Maxillofac Implants, 2001. **16**(2): p. 193-200.

45. Mendonca, G., et al., *Advancing dental implant surface technology--from micron- to nanotopography.* Biomaterials, 2008. **29**(28): p. 3822-35.

46. Dohan Ehrenfest, D.M., et al., *Classification of osseointegrated implant surfaces: materials, chemistry and topography.* Trends Biotechnol, 2010. **28**(4): p. 198-206.

47. Le Guehennec, L., et al., *Surface treatments of titanium dental implants for rapid osseointegration.* Dent Mater, 2007. **23**(7): p. 844-54.

48. Ivanoff, C.J., et al., *Histologic evaluation of the bone integration of TiO(2) blasted and turned titanium microimplants in humans.* Clin Oral Implants Res, 2001. **12**(2): p. 128-34.

49. Aparicio, C., et al., *Corrosion behaviour of commercially pure titanium shot blasted with different materials and sizes of shot particles for dental implant applications.* Biomaterials, 2003. **24**(2): p. 263-73.

50. van Steenberghe, D., et al., *A prospective split-mouth comparative study of two screw-shaped self-tapping pure titanium implant systems.* Clin Oral Implants Res, 2000. **11**(3): p. 202-9.

51. Galli, C., et al., *Comparison of human mandibular osteoblasts grown on two commercially available titanium implant surfaces.* J Periodontol, 2005. **76**(3): p. 364-72.

52. Kasemo, B. and J. Gold, *Implant surfaces and interface processes.* Adv Dent Res, 1999. **13**: p. 8-20.

53. Rupp, F., et al., *Wetting behavior of dental implants.* Int J Oral Maxillofac Implants, 2011. **26**(6): p. 1256-66.

54. Israelachvili, J. and H. Wennerstrom, *Role of hydration and water structure in biological and colloidal interactions.* Nature, 1996. **379**(6562): p. 219-25.

55. Higuchi, A., et al., *Chemically modified polysulfone hollow fibers with vinylpyrrolidone having improved blood compatibility.* Biomaterials, 2002. **23**(13): p. 2659-66.

56. Hess, H. and V. Vogel, *Molecular shuttles based on motor proteins: active transport in synthetic environments.* J Biotechnol, 2001. **82**(1): p. 67-85.

57. MacDonald, D.E., et al., *Adsorption and dissolution behavior of human plasma fibronectin on thermally and chemically modified titanium dioxide particles.* Biomaterials, 2002. **23**(4): p. 1269-79.

58. Shen, M., et al., *Effects of adsorbed proteins and surface chemistry on foreign body giant cell formation, tumor necrosis factor alpha release and procoagulant activity of monocytes.* J Biomed Mater Res A, 2004. **70**(4): p. 533-41.

59. Anderson, J.M., T.L. Bonfield, and N.P. Ziats, *Protein adsorption and cellular adhesion and activation on biomedical polymers.* Int J Artif Organs, 1990. **13**(6): p. 375-82.

60. Andrade, J.D. and V. Hlady, *Plasma protein adsorption: the big twelve.* Ann N Y Acad Sci, 1987. **516**: p. 158-72.

61. Thevenot, P., W. Hu, and L. Tang, *Surface chemistry influences implant biocompatibility.* Curr Top Med Chem, 2008. **8**(4): p. 270-80.

62. Aita, H., et al., *The effect of ultraviolet functionalization of titanium on integration with bone.* Biomaterials, 2009. **30**(6): p. 1015-25.

63. Att, W., et al., *Time-dependent degradation of titanium osteoconductivity: an implication of biological aging of implant materials.* Biomaterials, 2009. **30**(29): p. 5352-63.

64. Att, W., et al., *The effect of UV-photofunctionalization on the time-related bioactivity of titanium and chromium-cobalt alloys.* Biomaterials, 2009. **30**(26): p. 4268-76.

65. Kasemo, B. and J. Lausmaa, *Biomaterial and implant surfaces: on the role of cleanliness, contamination, and preparation procedures.* J Biomed Mater Res, 1988. **22**(A2 Suppl): p. 145-58.

66. Att, W. and T. Ogawa, *Biological aging of implant surfaces and their restoration with ultraviolet light treatment: a novel understanding of osseointegration.* Int J Oral Maxillofac Implants, 2012. **27**(4): p. 753-61.

67. Ueno, T., et al., *Effect of ultraviolet photoactivation of titanium on osseointegration in a rat model.* Int J Oral Maxillofac Implants, 2010. **25**(2): p. 287-94.

68. Lee, J.H. and T. Ogawa, *The biological aging of titanium implants.* Implant Dent, 2012. **21**(5): p. 415-21.

69. Hori, N., et al., *Age-dependent degradation of the protein adsorption capacity of titanium.* J Dent Res, 2009. **88**(7): p. 663-7.

70. Morra, M., et al., *Surface chemistry effects of topographic modification of titanium dental implant surfaces: 1. Surface analysis.* Int J Oral Maxillofac Implants, 2003. **18**(1): p. 40-5.

71. Kazuhito, H., I. Hiroshi, and F. Akira, *TiO 2 Photocatalysis: A Historical Overview and Future Prospects.* Japanese Journal of Applied Physics, 2005. **44**(12R): p. 8269.

72. Egerton, T.A., *UV-absorption--the primary process in photocatalysis and some practical consequences.* Molecules, 2014. **19**(11): p. 18192-214.

73. Suzuki, T., et al., *Ultraviolet treatment overcomes time-related degrading bioactivity of titanium.* Tissue Eng Part A, 2009. **15**(12): p. 3679-88.

74. Hori, N., et al., *Ultraviolet light treatment for the restoration of age-related degradation of titanium bioactivity.* Int J Oral Maxillofac Implants, 2010. **25**(1): p. 49-62.

75. Aita, H., et al., *Ultraviolet light-mediated photofunctionalization of titanium to promote human mesenchymal stem cell migration, attachment, proliferation and differentiation.* Acta Biomater, 2009. **5**(8): p. 3247-57.

76. Ueno, T., et al., *Enhancement of bone-titanium integration profile with UV-photofunctionalized titanium in a gap healing model.* Biomaterials, 2010. **31**(7): p. 1546-57.

77. Ogawa, T., *Ultraviolet photofunctionalization of titanium implants.* Int J Oral Maxillofac Implants, 2014. **29**(1): p. e95-102.

78. Iwasa, F., et al., *Enhancement of osteoblast adhesion to UV-photofunctionalized titanium via an electrostatic mechanism.* Biomaterials, 2010. **31**(10): p. 2717-27.

79. Hori, N., et al., *Effects of UV photofunctionalization on the nanotopography enhanced initial bioactivity of titanium.* Acta Biomater, 2011. **7**(10): p. 3679-91.

80. Tsukimura, N., et al., *Synergistic effects of UV photofunctionalization and micro-nano hybrid topography on the biological properties of titanium.* Biomaterials, 2011. **32**(19): p. 4358-68.

81. Giordano, A., U. Galderisi, and I.R. Marino, *From the laboratory bench to the patient's bedside: an update on clinical trials with mesenchymal stem cells.* J Cell Physiol, 2007. **211**(1): p. 27-35.

82. Caplan, A.I., *Adult mesenchymal stem cells for tissue engineering versus regenerative medicine.* J Cell Physiol, 2007. **213**(2): p. 341-7.

83. Fox, J.M., et al., *Recent advances into the understanding of mesenchymal stem cell trafficking.* Br J Haematol, 2007. **137**(6): p. 491-502.

84. Seah, M.P., *Quantitative Auger electron spectroscopy: Via the energy spectrum or the differential?* Surface and Interface Analysis, 1979. **1**(3): p. 86-90.

85. Kang, B.S., et al., *XPS, AES and SEM analysis of recent dental implants.* Acta Biomater, 2009. **5**(6): p. 2222-9.

86. John F. Moulder, W.F.S., Peter E. Sobol, Kenneth D. Bomben, *Handbook of X-ray Photoelectron Spectroscopy.* 1995: p. 255.

87. Picchi, J., et al., *HOX and TALE signatures specify human stromal stem cell populations from different sources.* J Cell Physiol, 2013. **228**(4): p. 879-89.

88. Buser, D., et al., *Influence of surface characteristics on bone integration of titanium implants. A histomorphometric study in miniature pigs.* J Biomed Mater Res, 1991. **25**(7): p. 889-902.

89. Passeri, G., et al., *Adhesion pattern and growth of primary human osteoblastic cells on five commercially available titanium surfaces.* Clin Oral Implants Res, 2010. **21**(7): p. 756-65.

90. Cordioli, G., et al., *Removal torque and histomorphometric investigation of 4 different titanium surfaces: an experimental study in the rabbit tibia.* Int J Oral Maxillofac Implants, 2000. **15**(5): p. 668-74.

91. Klokkevold, P.R., et al., *Osseointegration enhanced by chemical etching of the titanium surface. A torque removal study in the rabbit.* Clin Oral Implants Res, 1997. **8**(6): p. 442-7.

92. Cochran, D.L., et al., *Bone response to unloaded and loaded titanium implants with a sandblasted and acid-etched surface: a histometric study in the canine mandible.* J Biomed Mater Res, 1998. **40**(1): p. 1-11.

93. Offermanns, V., et al., *A comparative in vivo study of strontium-functionalized and SLActive implant surfaces in early bone healing.* Int J Nanomedicine, 2018. **13**: p. 2189-2197.

94. De Maeztu, M.A., et al., *Improvement of osseointegration of titanium dental implant surfaces modified with CO ions: a comparative histomorphometric study in beagle dogs.* Int J Oral Maxillofac Surg, 2008. **37**(5): p. 441-7.

95. Roy, M., et al., *Photofunctionalization of Titanium: An Alternative Explanation of Its Chemical-Physical Mechanism.* PLoS One, 2016. **11**(6): p. e0157481.

96. Elias, C.N., et al., *Relationship between surface properties (roughness, wettability and morphology) of titanium and dental implant removal torque.* J Mech Behav Biomed Mater, 2008. **1**(3): p. 234-42.

97. Chai, F., et al., *Osteoblast interaction with DLC-coated Si substrates.* Acta Biomater, 2008. **4**(5): p. 1369-81.

98. Zhao, G., et al., *High surface energy enhances cell response to titanium substrate microstructure.* J Biomed Mater Res A, 2005. **74**(1): p. 49-58.

99. Yanagisawa, I., et al., *Effects of "wettability" of biomaterials on culture cells.* The Journal of oral implantology, 1989. **15**(3): p. 168-177.

100. Y. Oshida, R.S., S. Miyazaki, J. Daly, *effects of shot peening on surface contact angles of biomaterials.* journal of materials science: materials in medicine, 1993. **4**: p. 5.

101. Kevin E. Healy, P.D., *Hydration and preferential adsorption on titanium in vitro.* Biomaterials, 1992. **13**(8): p. 9.

102. Jackman, M.J., A.G. Thomas, and C. Muryn, *Photoelectron Spectroscopy Study of Stoichiometric and Reduced Anatase TiO2(101) Surfaces: The Effect of Subsurface Defects on Water Adsorption at Near-Ambient Pressures.* The Journal of Physical Chemistry C, 2015. **119**(24): p. 13682-13690.

103. Castellote, M. and N. Bengtsson, *Principles of TiO2 Photocatalysis*, in *Applications of Titanium Dioxide Photocatalysis to Construction Materials*, Y. Ohama and D. Van Gemert, Editors. 2011, Springer Netherlands. p. 5-10.

104. Stein, G.S. and J.B. Lian, *Molecular mechanisms mediating proliferation/differentiation interrelationships during progressive development of the osteoblast phenotype.* Endocr Rev, 1993. **14**(4): p. 424-42.

105. Owen, T.A., et al., *Progressive development of the rat osteoblast phenotype in vitro: reciprocal relationships in expression of genes associated with osteoblast proliferation and differentiation during formation of the bone extracellular matrix.* J Cell Physiol, 1990. **143**(3): p. 420-30.

106. Ogawa, T., C. Sukotjo, and I. Nishimura, *Modulated bone matrix-related gene expression is associated with differences in interfacial strength of different implant surface roughness.* J Prosthodont, 2002. **11**(4): p. 241-7.

107. Ogawa, T. and I. Nishimura, *Different bone integration profiles of turned and acid-etched implants associated with modulated expression of extracellular matrix genes.* Int J Oral Maxillofac Implants, 2003. **18**(2): p. 200-10.

108. Bachle, M. and R.J. Kohal, *A systematic review of the influence of different titanium surfaces on proliferation, differentiation and protein synthesis of osteoblast-like MG63 cells.* Clin Oral Implants Res, 2004. **15**(6): p. 683-92.

109. Singh, M., C. Berkland, and M.S. Detamore, *Strategies and Applications for Incorporating Physical and Chemical Signal Gradients in Tissue Engineering.* Tissue Engineering. Part B, Reviews, 2008. **14**(4): p. 341-366.

110. Washburn, N.R., et al., *High-throughput investigation of osteoblast response to polymer crystallinity: influence of nanometer-scale roughness on proliferation.* Biomaterials, 2004. **25**(7-8): p. 1215-24.

111. Iwasa, F., et al., *TiO2 micro-nano-hybrid surface to alleviate biological aging of UV-photofunctionalized titanium.* Int J Nanomedicine, 2011. **6**: p. 1327-41.

112. Bar-Shavit, R., et al., *Thrombin as a multifunctional protein: induction of cell adhesion and proliferation.* Am J Respir Cell Mol Biol, 1992. **6**(2): p. 123-30.

113. M. Moursi, Ruth K. Globus, Caroline H. Damsky, *Interactions between integrin receptors and fibronectin are required for calvarial osteoblast differentiation in vitro.* Journal of Cell Science, 1997(110): p. 10.

114. García, A.J., M.D. Vega, and D. Boettiger, *Modulation of Cell Proliferation and Differentiation through Substrate-dependent Changes in Fibronectin Conformation.* Molecular Biology of the Cell, 1999. **10**(3): p. 785-798.

LIST OF FIGURES

LIST OF TABLES